Journal of General Virology (2005), 86, 2209–2220 DOI 10.1099/vir.0.80638-0

Characterization of the E-138 (Glu/Lys) mutation in *Japanese encephalitis virus* by using a stable, full-length, infectious cDNA clone

Zijiang Zhao,[1] Tomoko Date,[1] Yuhua Li,[2] Takanobu Kato,[1] Michiko Miyamoto,[1] Kotaro Yasui[1] and Takaji Wakita[1]

Correspondence
Takaji Wakita
wakita@tmin.ac.jp

[1]Department of Microbiology, Tokyo Metropolitan Institute for Neuroscience, 2-6 Musashidai, Fuchu-shi, Tokyo 183-8526, Japan

[2]Chengdu Institute of Biological Products, Chengdu 610063, Sichuan Province, PR China

A stable plasmid DNA, pMWJEAT, was constructed by using full-length *Japanese encephalitis virus* (JEV) cDNA isolated from the wild-type strain JEV AT31. Recombinant JEV was obtained by synthetic RNA transfection into Vero cells and designated rAT virus. JEV rAT exhibited similar large-plaque morphology and antigenicity to the parental AT31 strain. Mutant clone pMWJEAT-E138K, containing a single Glu-to-Lys mutation at aa 138 of the envelope (E) protein, was also constructed to analyse the mechanisms of viral attenuation arising from this mutation. Recombinant JEV rAT-E138K was also recovered and displayed a smaller-plaque morphology and lower neurovirulence and neuroinvasiveness than either AT31 virus or rAT virus. JEV rAT-E138K exhibited greater plaque formation than rAT virus in virus–cell interactions under acidic conditions. Heparin or heparinase III treatment inhibited binding to Vero cells more efficiently for JEV rAT-E138K than for rAT virus. Inhibition of virus–cell interactions by using wheatgerm agglutinin was more effective for JEV rAT than for rAT-E138K on Vero cells. About 20 % of macropinoendocytosis of JEV rAT for Vero cells was inhibited by cytochalasin D treatment, but no such inhibition occurred for rAT-E138K virus. Furthermore, JEV rAT was predominantly secreted from infected cells, whereas rAT-E138K was more likely to be retained in infected cells. This study demonstrates clearly that a single Glu-to-Lys mutation at aa 138 of the envelope protein affects multiple steps of the viral life cycle. These multiple changes may induce substantial attenuation of JEV.

Received 25 September 2004
Accepted 21 April 2005

INTRODUCTION

Japanese encephalitis virus (JEV) belongs to the genus *Flavivirus*, which predominantly comprises arthropod-borne viruses. Members of this genus are distributed throughout the world. JEV has a single-strand, positive-sense RNA genome of approximately 11 000 nt, which is translated from a single open reading frame into a polyprotein that is processed by viral and host proteases to yield three structural proteins [capsid, membrane or precursor membrane (prM) and envelope (E)] encoded at the 5′ end of the genome, followed by at least seven non-structural proteins (Monath & Heinz, 1996). The flavivirus E protein is the viral haemagglutinin, which induces protective immunity and mediates receptor-specific virus attachment to cell surfaces (Kimura-Kuroda & Yasui, 1983). The E protein plays major roles in determining viral pathogenicity by defining cellular tropism and affecting penetration into susceptible cells (Heinz, 1986; Mandl *et al.*, 1989). X-ray crystallographic resolution of the structure of the E ectodomain in *Tick-borne encephalitis virus* (TBE virus) reveals that the E protein forms head-to-tail homodimers that lie parallel to the viral envelope (Rey *et al.*, 1995). These homodimers dissociate, leading to irreversible formation of homotrimers on the surface of viral particles under conditions of low pH (Allison *et al.*, 1995; Kuhn *et al.*, 2002; Stiasny *et al.*, 2002).

Studies attempting to elucidate the molecular basis of JEV attenuation have analysed the genomes of both the virulent parental strain SA14 and the attenuated vaccine virus SA14-14-2 (Nitayaphan *et al.*, 1990; Aihara *et al.*, 1991). Several JEV mutants have been obtained through γ-ray irradiation (Chen *et al.*, 1996) or passage in cultured cells (Hasegawa *et al.*, 1992). These studies have indicated that some mutations in the E protein correlate with viral attenuation, including the amino acid mutation from glutamic acid (Glu) to lysine (Lys) at residue 138 of the E protein (E-138). Due to the multiple mutations present, the

The GenBank/EMBL/DDBJ accession numbers for the sequences described in this study are given in Table 1.

Supplementary figures and tables are available in JGV Online.

exact mutated residue changes in the E protein that are primarily responsible for JEV attenuation are not clearly understood. Since infectious *Yellow fever virus* RNA was transcribed successfully from a full-length cDNA template by using *in vitro* ligation of two cDNA fragments (Rice *et al.*, 1989), infectious flavivirus clones have been constructed in similar fashion for JEV (Sumiyoshi *et al.*, 1992), dengue virus type 2 (Polo *et al.*, 1997; Gualano *et al.*, 1998), dengue virus type 4 (Lai *et al.*, 1991) and other viruses (Khromykh & Westaway, 1994; Gritsun & Gould, 1998; Shi *et al.*, 2002; Hayasaka *et al.*, 2004). This method seems valuable in studying biological function, polyprotein processing and virulence of mutant viruses with specific mutations in various regions of the viral genome. However, irregular mutations occur frequently in full-length JEV cDNA clones during cloning into plasmid vectors, particularly in the 5′ fragment, and this has seriously affected such studies (Sumiyoshi *et al.*, 1995; Yamshchikov *et al.*, 2001). Specific strategies are thus necessary to establish stable, full-length JEV infectious clones, such as insertion of short introns or cloning into bacterial artificial chromosomes (Yamshchikov *et al.*, 2001; Yun *et al.*, 2003).

The present report describes the construction of a stable, full-length cDNA clone of the wild-type JEV AT31 strain into the very low-copy-number plasmid pMW118 by using conventional molecular-cloning technology. Another plasmid, containing a Glu-to-Lys mutation at the E-138 residue, was also constructed. Recombinant JEVs comprising wild-type and mutant viruses were recovered after synthetic RNA transfection, and were characterized with regard to viral virulence, internalization and release.

METHODS

Cells, viruses, antibodies and mice. Vero cells and C6/36 cells were maintained in Eagle's minimum essential medium (MEM) supplemented with 5% fetal calf serum (FCS). Primary neural cells from cerebral cortices of embryonic BALB/c mice at gestational day 18 (Japan SLC) were maintained as described previously (Wilcox *et al.*, 1990).

The wild-type JEV strain AT31 was a gift from Dr Nakamura of the Nippon Institute for Biological Science, Japan. Attenuated JEV at222 strain was obtained after 222 passages through primary hamster kidney cells to obtain a vaccine strain, as described previously (Yasui, 2002). Recombinant wild-type rAT virus and mutant rAT-E138K were obtained from supernatants of Vero cells transfected with *in vitro*-transcribed RNAs. All cDNA sequences of viral RNAs were determined and deposited in GenBank/DDBJ/EMBL (Table 1). The at222 strain contains several mutations, including the Glu-to-Lys mutation at residue E-138. All viruses were propagated once in Vero cells or C6/36 cells and supernatants were obtained and stored at −80 °C until used. Three-day-old BALB/c mice were inoculated intracerebrally with 10^4 p.f.u. JEV rAT-E138K. The inoculated mice were sacrificed at 8 days of age and their brains were harvested and homogenized. Reverted virus RE-138 was recovered from a single large plaque on Vero cells inoculated with the supernatant of homogenized brains. Rabbit anti-JEV serum was prepared as described previously (Kimura-Kuroda *et al.*, 1993).

BALB/c mice were purchased from Japan SLC Inc. All mice were maintained in pathogen-free environments. All experiments were conducted in accordance with the Guidelines for the Care and Use of Animals, 2000 (Tokyo Metropolitan Institute for Neuroscience, Tokyo, Japan).

Construction of full-length cDNA and a point-mutant cDNA of JEV strain AT31. RNA was extracted from the supernatant of C6/36 cells infected with AT31 by using Isogen-LS (Nippon Gene). Oligonucleotide primers were designed based on sequence data for JEV strain JaOArS982 (GenBank/EMBL/DDBJ accession no. M18370; Sumiyoshi *et al.*, 1987) and the sequences of these primers are listed in Supplementary Table S1 (available in JGV Online). The RNA solution was subjected to reverse transcription (RT) using an antisense primer, JEV-10976R-30, and Moloney murine leukemia virus reverse transcriptase (Superscript II; Invitrogen) at 42 °C for 1 h. Both 5′ and 3′ fragments of JEV cDNA (nt 1–6125 and 5383–10976, respectively) were amplified by using two pairs of primers: SalT7GJE5P20S and JEV-6125R-30 for the 5′ fragment or JEV-5383S-30 and ClaKpnJE3P30R for the 3′ fragment, with TaKaRa LA *Taq* polymerase. PCR conditions comprised 30 cycles of denaturing

Table 1. Origin, sequence, neurovirulence and neuroinvasiveness of JEV in this study

NA, Not applicable; ND, not done.

Virus	Origin	Sequence accession no.*	Neurovirulence† (p.f.u./LD_{50})	Neuroinvasiveness‡ (p.f.u./LD_{50})
AT31	Parent	AB196923	2·2	18 800
at222	Vaccine	AB196924	148 000	$>10^7$
rAT§	Recombinant‖	AB196925	2·5	24 200
rAT-E138K¶	Recombinant‖	AB196926	15 200	$>10^7$
RE-138	Reverted	NA	2·2	ND

*Sequences in GenBank/DDBJ/EMBL.

†Intracerebral inoculation with 0·025 ml virus solution in 3-week-old female BALB/c mice.

‡Intraperitoneal inoculation with 0·1 ml virus solution in 3-week-old female BALB/c mice.

§Transcribed RNA prepared from pMWJEAT.

‖Recombinant virus obtained by RNA transfection.

¶Transcribed RNA prepared from pMWJEAT-E138K.

at 95 °C for 10 s and annealing and extension at 68 °C for 6 min. PCR products containing 5′ and 3′ fragments of JEV cDNA were cloned into pBR322. Three cloned plasmids were selected for further reconstruction of a full-length JEV cDNA: pJEAT-5′-132 contained the 5′ end to the *Sac*I site (nt 2215) region; pJEAT-5′-258 contained the *Sac*I site (nt 2215) to *Bam*HI site (nt 5576) region; and pJEAT-3′-75 contained the *Bam*HI site (nt 5576) to 3′ end region (see Supplementary Fig. S1, available in JGV Online). For subcloning purposes, the second *Sac*I site in JEV cDNA was abolished by using PCR-based mutagenesis (Kato *et al.*, 2003a), with an A-to-T mutation at nt 6713 of pJEAT-3′-75, producing pJEAT-3′-75dSac. Each insert from pJEAT-5′-132, pJEAT-5′-258 and pJEAT-3′-75dSac was cloned stably into a very low-copy-number plasmid vector, pMW118 (Nippon Gene), to construct the full-length JEV cDNA and the result was designated pMWJEAT (see Supplementary Fig. S1, available in JGV Online). A single G-to-A point mutation at nt 1389 was also introduced into pMWJEAT by PCR-based mutagenesis and designated pMWJEAT-E138K (Fig. 1a).

Transfection of synthetic JEV RNA into Vero cells by electroporation. Plasmid DNAs pMWJEAT and pMWJEAT-E138K were digested by using *Kpn*I. JEV RNA was synthesized by using a MEGAscript T7 kit (Ambion) and treated with DNase I (RQ1 RNase-free DNase; Promega) followed by acid–phenol extraction (Kato *et al.*, 2003b). Trypsinized Vero cells were washed by using Opti-MEM I (Invitrogen) and resuspended in Cytomix buffer at $7{\cdot}5 \times 10^6$ cells ml^{-1} (Kato *et al.*, 2003b). Synthesized RNA (10 μg) mixed with 400 μl cell suspension was pulsed at 260 V and 950 μF by using a Gene Pulser II apparatus (Bio-Rad).

Plaque-reduction neutralization (PRNT) test. The PRNT test was done as described previously (Zhao *et al.*, 2003). PRNT titre was expressed as the maximum dilution of antibody yielding a 90% reduction in viral infectivity ($PRNT_{90}$).

Mouse experiments. Groups of 3-week-old female BALB/c mice ($n=5$) were inoculated intracerebrally with 25 μl of a tenfold serially diluted virus solution (AT31, at222, rAT, rAT-E138K and RE-138). Similar groups of mice were inoculated intraperitoneally with 0·1 ml of a tenfold serially diluted virus solution. Mice were observed for 3 weeks after inoculation. End points of neurovirulence and neuroinvasiveness were identified as both mortality ratios and mean survival times. The LD_{50} was determined for each virus (Reed & Muench, 1938).

Groups of 3-week-old female BALB/c mice ($n=30$) were inoculated with 10^5 p.f.u. rAT in 25 μl or 10^7 p.f.u. rAT-E138K in 25 μl into the left footpad. At 2-day intervals after inoculation, two mice from each group were bled periorbitally before cardiac perfusion with HBSS solution (Invitrogen). Brains, livers, spleens and kidneys of mice were harvested. Tissue suspensions of 10% (w/v) were prepared by using PBS, then homogenized immediately. After three cycles of freezing and thawing, these 10% (w/v) tissue suspensions were centrifuged at 20 000 *g* at 4 °C for 1 h, then filtered through a 0·2 μm filter. Virus titres in filtered supernatant were determined by plaque assay on Vero cells.

Acid resistance of early virus–cell interactions. Vero cells (1×10^5) cultured in a six-well tissue-culture plate (Corning) were washed and pre-chilled at 4 °C for 2 h. After inoculation with 400 p.f.u. virus (m.o.i., 0·004 p.f.u. per cell) at 4 °C for 2 h,

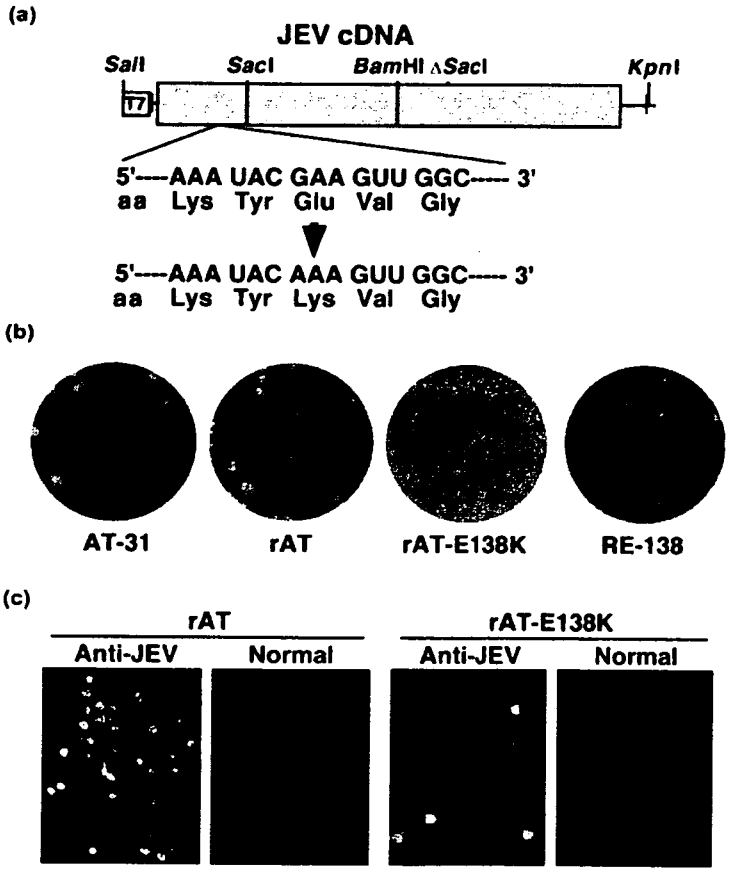

Fig. 1. (a) Schematic representation of the single point mutation in the full-length cDNA pMWJEAT-E138K of JEV AT31 strain, designated rAT-E138K strain. (b) Plaque morphology of wild-type virus AT31, recombinant virus rAT, mutant virus rAT-E138K and reverted virus RE-138. Vero cells infected with virus were fixed in 10% formalin/PBS solution and stained by using 0·1% crystal violet solution. (c) Detection of recombinant JEV rAT and rAT-E138K in the cerebral cortex of 3-week-old female BALB/c mice by using IFA, as described in Methods. Positive signals were observed in neuron-like cells in the cerebral cortex of rAT- and rAT-E138K-infected mice.

unbound virus was removed by washing three times with ice-cold MEM supplemented with 2% FCS (MEM-2). Cells were treated with 2 ml glycine/HCl-buffered saline (8 g NaCl, 0·38 g KCl, 0·10 g $MgCl_2.6H_2O$, 0·10 g $CaCl_2.2H_2O$ and 7·5 g glycine l^{-1}, pH adjusted to 3·0 with HCl) at room temperature for 5 min, as described by Hung *et al.* (1999), then overlaid with 1·25% methyl cellulose/MEM for incubation at 37 °C for 5 days. Infected cells without acid treatment were used as controls. Penetration rates of acid-resistant intracellular viruses were calculated as 100× [no. plaques (acid-treated)/no. plaques (controls)].

Heparin assay and heparinase-treatment effect on Vero cells. Inhibition of JEV binding to Vero cells by heparin (Sigma) was performed as described by Hung *et al.* (1999), with some modifications. The following two conditions were tested: (i) 400 p.f.u. virus plus heparin was pre-incubated at 37 °C for 1 h, then incubated in Vero cells cultured in a six-well plate at 37 °C for 2 h; and (ii) in total, 400 p.f.u. virus was reacted with heparin at 37 °C for 1 h, then inoculated into Vero cells at 4 °C for 2 h. Unbound virus was removed by three washes with MEM-2. Cells were overlaid with 1·25% methyl cellulose/MEM to incubate at 37 °C for 5 days. Cells inoculated by using the same procedure without heparin were used as controls. Inhibition was described as: 100× [no. plaques (heparin treatment)/no. plaques (controls)].

The effectiveness of heparinase treatment was analysed on Vero cells that had been treated with different concentrations of heparinase I or III (Sigma Aldrich) at 37 °C for 1 h. Cells cultured in a six-well plate were pre-chilled at 4 °C for 1 h after washing and inoculated with 400 p.f.u. per well (m.o.i., 0·004 p.f.u. per cell) of JEV rAT or rAT-E138K at 4 °C for 2 h. After washing in MEM-2, cells were overlaid with methyl cellulose and incubated at 37 °C for 5 days. Cells not treated with heparinase were used as controls. Inhibition was calculated as described above.

Binding inhibition of recombinant JEV with lectins. The ability of rAT and rAT-E138K to bind to Vero cells was examined by using concanavalin A (ConA; Sigma), wheatgerm agglutinin (WGA; Sigma) and phytohaemagglutinin P (PHA-P; Sigma) as described by Hung *et al.* (1999). A total of 400 p.f.u. virus was reacted with lectin at 37 °C for 1 h, then inoculated into Vero cells cultured in a six-well plate for 2 h. After washing in MEM-2, cells were overlaid with methyl cellulose and incubated at 37 °C for 5 days. Cells inoculated by using viral solutions without lectin were used as controls. Inhibition was calculated as: 100× [no. plaques (lectin treatment)/no. plaques (controls)].

Endocytosis inhibition. Inhibition of rAT and rAT-E138K virus internalization into Vero cells was analysed by using different concentrations of chlorpromazine, cytochalasin D or nystatin (all from Sigma). Vero cells cultured in a six-well plate were treated with these reagents at 37 °C for 1·5 h. These cells were subsequently inoculated with 400 p.f.u. JEV at 37 °C for another 3 h in the presence of the reagents, followed by treatment with glycine/HCl-buffered saline at room temperature for 5 min to inactivate unpenetrated viruses on the cell surface. Inoculated cells without any inhibiting agent were used as controls. Inhibition was calculated as: 100× [no. plaques (agent treatment)/no. plaques (controls)].

Immunohistochemistry. BALB/c mice (3 weeks old; $n=5$) received inoculation with 10 p.f.u. JEV rAT or 10^5 p.f.u. rAT-E138K into the right cerebral hemisphere. Virus titres were detected in the right hemispheres of sacrificed moribund mice. Left hemispheres were embedded immediately in Tissue-Tek embedding medium (Sakura Finetechnical) to examine the presence of JEV antigen with rabbit anti-JEV serum by using an immunofluorescence assay (IFA) as described previously (Zhao *et al.*, 2003).

Statistical analysis. Statistical analysis was performed by using Student's *t*-test. Survival rates of inoculated mice were analysed by using Kaplan–Meier methods. Values of $P<0·05$ were considered statistically significant.

RESULTS

Construction of a single plasmid DNA containing full-length JEV cDNA

Cloning a full-length JEV cDNA into a single plasmid vector, such as pUC or even a low-copy-number plasmid vector like pBR322 (Sumiyoshi *et al.*, 1992), is difficult without the insertion of short introns (Yamshchikov *et al.*, 2001). We thought that this difficulty might be attributable to toxicity of the proteins produced by JEV cDNA in transformed bacterial cells. To reduce this toxicity, we cloned full-length JEV cDNA into the very low-copy-number vector pMW118, a derivative of pSC101 (see Supplementary Fig. S1, available in JGV Online). The resultant plasmid, pMWJEAT, contained a full-length cDNA of the JEV AT31 strain and was amplified stably in bacterial cells. A mutant plasmid, pMWJEAT-E138K, containing a single Glu-to-Lys point mutation at aa 138 of the E protein, was also constructed (Fig. 1a).

Generation of recombinant JEV on Vero and C6/36 cells

The cDNA-generated recombinant JEV strains rAT and rAT-E138K were obtained from the supernatant of Vero cells transfected with synthetic RNA using the full-length cDNA clone as described in Methods. Viral RNA was extracted from both rAT and rAT-E138K virus solutions and sequences were determined directly after RT-PCR. No mutations were found in the genomic sequences as compared with template plasmid DNA sequences. Parental wild-type AT31 and recombinant rAT viruses displayed similar plaque morphologies at 5 days after infection (diameter ~3·1 mm), whereas rAT-E138K virus exhibited a smaller-plaque morphology (diameter ~0·45 mm) on Vero cells (Fig. 1b). Plaques similar to those of rAT-E138K were observed in all supernatant samples following seven passages on C6/36 cells. Reverted RE-138 virus was obtained as described in Methods. RE-138 virus also exhibited larger-size plaques (~3·1 mm) than those of AT31 and rAT viruses, as shown in Fig. 1(b).

Neurovirulence and neuroinvasiveness of recombinant JEV

Neurovirulence and neuroinvasiveness of JEV strains were determined by direct intracerebral inoculation or intraperitoneal infection using the tested viruses obtained from the supernatants of infected cells, as described in Methods. The JEV rAT strain displayed strong neurovirulence in 3-week-old BALB/c mice, as did the parent AT31 (2·5 and 2·2 p.f.u./LD_{50}, respectively; Table 1). In contrast, the rAT-E138K strain displayed much lower neurovirulence in mice

(15 200 p.f.u./LD_{50}) and the attenuated JEV at222 strain displayed the lowest neurovirulence (148 000 p.f.u./LD_{50}). However, RE-138 virus reverted from the rAT-E138K strain displayed strong neurovirulence (2·2 p.f.u./LD_{50}; Table 1), comparable to that seen with rAT and AT31 virus. After sequence analysis of RE-138 virus from the supernatant of infected Vero cells, only residue E-138 had been changed from Lys to Glu, compared with the rAT-E138K virus (data not shown). Furthermore, the JEV rAT strain demonstrated strong neuroinvasiveness, comparable to that of the parental AT31 strain (18 800 and 24 200 p.f.u./LD_{50}, respectively). Both rAT-E138K and at222 strains exhibited weak neuroinvasiveness ($>10^7$ p.f.u./LD_{50} for both strains), as all mice inoculated with 10^7 p.f.u. of either rAT-E138K or at222 survived (Table 1). These results demonstrate that the Glu-to-Lys mutation at residue E-138 of the JEV AT31 strain strongly attenuates viral neurovirulence and neuroinvasiveness in BALB/c mice.

Detection of JEV antigen in inoculated mouse brain

Positive signals were detected in both rAT- and rAT-E138K-infected mouse brains by IFA, and most positive cells displayed a neuronal morphology (Fig. 1c). The majority of positive signals were distributed in both the cerebral cortex and putaminal areas in brains of rAT-infected mice, whereas most positive cells were present in the frontal area of the cerebral cortex in rAT-E138K-infected mice. No positive signals were identified in the cerebella of either rAT- or rAT-E138K-infected mice (data not shown). These results indicate that the point mutation does not change viral neurotropism in BALB/c mice, although neurovirulence is attenuated.

JEV titre of infected mouse tissues

All mice inoculated with 10^7 p.f.u. rAT-E138K into the left footpad remained asymptomatic until 14 days post-inoculation, and no virus replication was detected in any tested tissue (Table 2). In contrast, viraemia (163 p.f.u. ml^{-1}) was detected in sera of mice inoculated with 10^5 p.f.u. of the rAT strain via the footpad on day 2 post-inoculation. Detectable levels of replicated rAT virus in brains of inoculated mice were identified at about $1·2 \times 10^4$ p.f.u. per tissue at 4 days post-inoculation, increasing to $8·6 \times 10^7$ p.f.u. per tissue by day 8. No virus was detected in any other tissue (Table 2).

Alteration in acid-resistant viral attachment by Glu-to-Lys mutation at E-138

Some flaviviruses display abolished infectivity with low-pH treatment after adsorption onto target cells (Hung *et al.*, 1999). We thus attached JEVs to Vero cells at 4 °C and then created conditions of low pH to determine the extent to which the adsorbed virus can maintain infectivity. Substantial reduction in plaque formation was detected in the rAT strain under conditions of low pH, with 7·79±2·31 % plaque formation compared with the control experiment (Fig. 2). However, rAT-E138K and at222 strains proved more resistant to low-pH treatment, with plaque formation at 35·95±9·61 and 34·83±4·19 %, respectively. These results indicate that the Glu-to-Lys mutation at E-138 alters the acid resistance of virus–cell attachment on Vero cells.

Table 2. Organ distribution of JEV in 3-week-old BALB/c mice inoculated with either 1×10^5 p.f.u. rAT or 1×10^7 p.f.u. rAT-E138K via the footpad

Virus	Virus titres in organ*				
	Serum	Brain	Kidney	Liver	Spleen
rAT					
0 d.p.i.†	−‡	−‡	−	−	−
2 d.p.i.	163	−	−	−	−
4 d.p.i.	−	$1·2 \times 10^4$	−	−	−
6 d.p.i.	−	$4·3 \times 10^7$	−	−	−
8 d.p.i.§	−	$8·6 \times 10^7$	−	−	−
rAT-E138K‖					
0 d.p.i.	−	−	−	−	−
14 d.p.i.	−	−	−	−	−

*Virus titre measured as p.f.u. ml^{-1} for serum, or p.f.u. per tissue for tissues.

†d.p.i., Days post-inoculation.

‡Virus titre, <25 p.f.u. ml^{-1} or <25 p.f.u. per tissue.

§Mice inoculated with 1×10^5 p.f.u. rAT were sacrificed at 8 days post-inoculation.

‖All mice inoculated with 1×10^7 p.f.u. rAT-E138K survived and no detectable virus (<25 p.f.u.) was identified in any tissues of mice sacrificed at 2-day intervals up to 14 days post-inoculation. Negative results at other days are not shown.

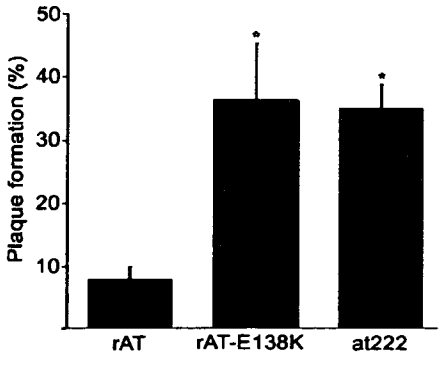

Fig. 2. Virus–cell interactions for recombinant JEV on Vero cells. Plaque-formation rates of rAT, rAT-E138K and attenuated at222 viruses bound to Vero cells at 4 °C were examined following treatment with glycine/HCl-buffered saline (pH 3·0) at room temperature for 5 min. Each value represents the mean of nine wells from three separate experiments. Error bars indicate SD. *, $P<0·01$.

Inhibition of virus–cell interactions with heparin or heparinase treatment

Both heparin and heparinase treatments have been used to inhibit the interactions of flavivirus and target cells (Chen *et al.*, 1997; Hung *et al.*, 1999). Infection by the rAT-E138K strain was clearly inhibited by heparin on Vero cells, whereas the rAT strain remained unaffected at both 4 and 37 °C (Fig. 3a, b). Significant differences in heparin inhibition between rAT and rAT-E138K were detected with heparin concentrations of 0·1–100 U ml^{-1} at 37 °C ($P<0·01$ or $P<0·001$; Fig. 3a) and of 0·1–1000 U ml^{-1} at 4 °C ($P<0·05$, $P<0·01$ or $P<0·001$; Fig. 3b), respectively. Similar results were noted on addition of heparin after virus attachment to Vero cells (data not shown).

Next, heparan sulphate on the surface of Vero cells was eliminated by treatment with heparinase I or III. Plaque formation for the JEV rAT strain on Vero cells was not inhibited by heparinase I or III treatment (Fig. 3c, d). However, plaque formation by rAT-E138K virus was reduced by both heparinase I and III (Fig. 3c, d). Differences in the plaque formation of infected Vero cells treated with heparinase I were small ($P<0·05$ at 4 U ml^{-1}; Fig. 3c). Treatment with >1 U heparinase III ml^{-1} on Vero cells reduced plaque formation of rAT-E138K by >40 %, but had no effect on rAT virus, representing a significant difference ($P<0·001$ for approx. 1–4 U heparinase III ml^{-1}; Fig. 3d). These data demonstrate that the point mutation increases dependency on heparan sulphate B residues for virus attachment to the cell surface.

Inhibition of virus–cell interactions with lectins

Regulation of viral entry by carbohydrates on dengue virus type 2 glycoproteins has been reported (Hung *et al.*, 1999). To explore the effect of the point mutation in JEV

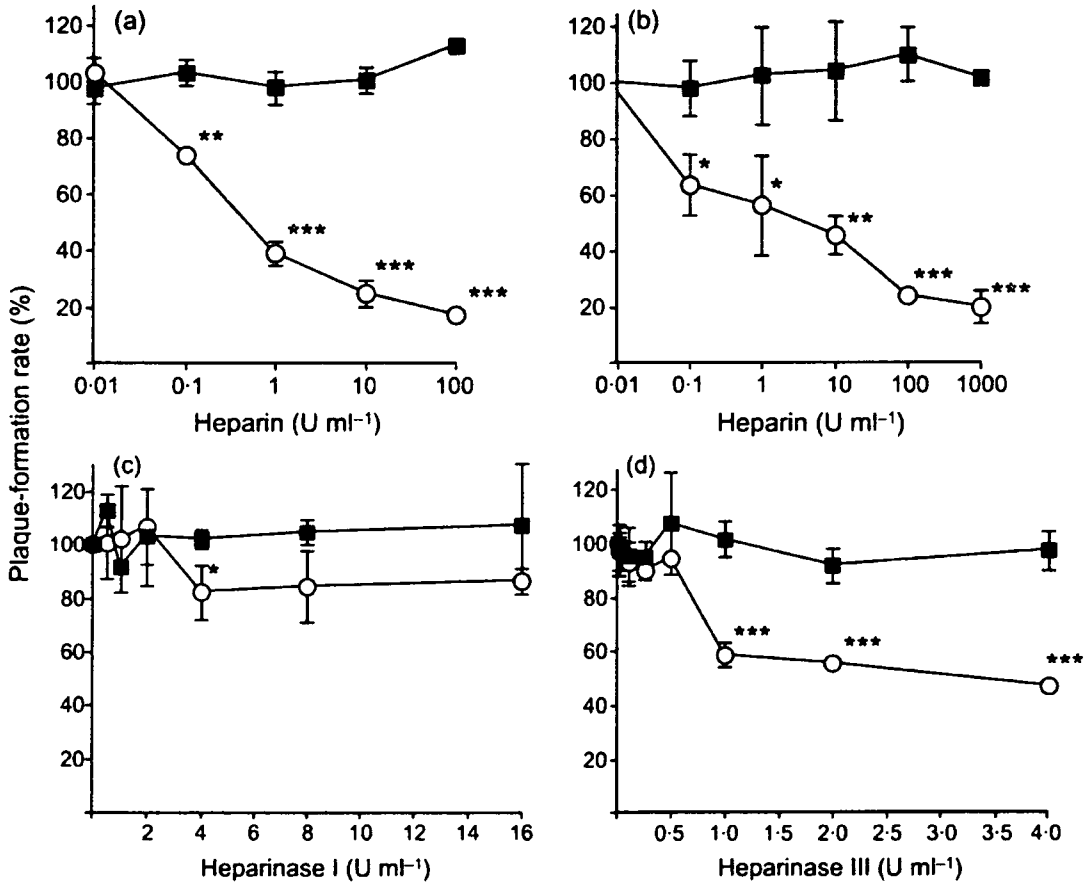

Fig. 3. Inhibition of recombinant JEV rAT (■) and rAT-E138K (○) plaque formation on Vero cells with heparan sulphate were analysed at 37 °C (a) and 4 °C (b). Plaque-formation rates of rAT (■) and rAT-E138K (○) viruses on Vero cells treated with heparinase I (c) or heparinase III (d) at 37 °C for 1 h were examined. Each value represents the mean of nine wells from three separate experiments. Error bars indicate SD. *, $P<0·05$; **, $P<0·01$; ***, $P<0·001$.

glycoproteins on this regulation, various lectins were used to inhibit virus–cell interactions. No significant differences in plaque formation were seen following ConA treatment between JEV rAT and rAT-E138K strain infection on Vero cells (Fig. 4a). However, significant differences in plaque formation were found between rAT and rAT-E138K strains when virus was treated with >5 μg WGA ml^{-1} pre-inoculation ($P<0{\cdot}01$ or $P<0{\cdot}001$; Fig. 4b). Finally, PHA-P did not reduce plaque formation in either JEV rAT or rAT-E138K strains at any tested concentration (Fig. 4c). These results indicate that the point mutation affects inhibition of virus–cell interactions with WGA, but exerts less effect with ConA and PHA-P. The higher efficiency of WGA inhibition against the rAT strain than against the rAT-E138K strain suggests that residues of β-*N*-acetylmuramic acid or α-*N*-acetylneuraminic acid on rAT virus are more involved in virus–cell interactions (Fig. 4b).

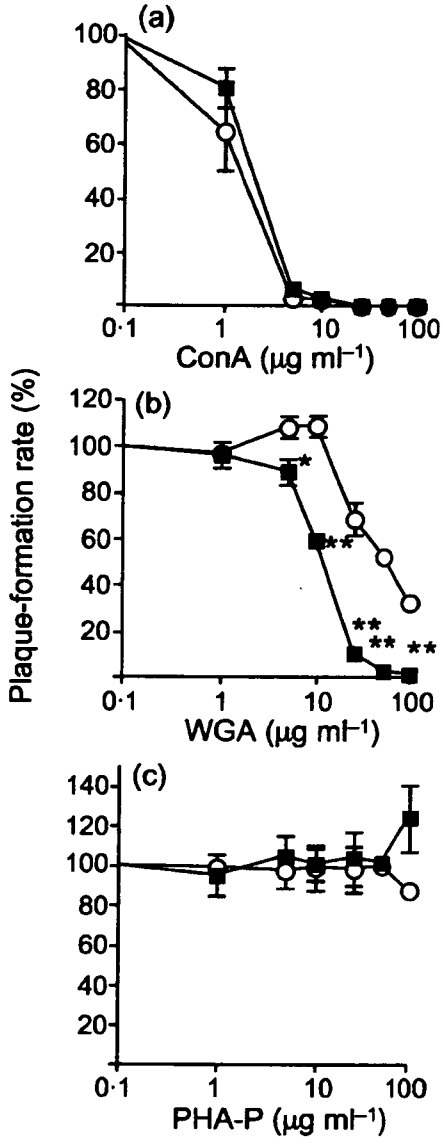

Fig. 4. Inhibition of viral internalization of rAT (■) and rAT-E138K (○) viruses into Vero cells with lectins: (a) concanavalin A; (b) wheatgerm agglutinin; and (c) phytohaemagglutinin P. Plaque-formation rates for each sample were examined. Each value represents the mean of three separate experiments. Error bars indicate SD. *, $P<0{\cdot}01$; **, $P<0{\cdot}001$.

Detection of endocytosis of recombinant JEV on Vero cells

Plaques of both rAT and rAT-E138K were effectively reduced by chlorpromazine on Vero cells (Fig. 5a). Plaque formation was inhibited more efficiently for rAT-E138K than for rAT at a concentration of 5 μg chlorpromazine ml^{-1} ($P<0{\cdot}05$). At a higher concentration of 20 μg ml^{-1}, about 20% of Vero cells dissociated due to cytotoxicity. This result indicates that clathrin-dependent endocytosis is involved in JEV infection. Plaque formation by rAT virus was reduced by about 20% by cytochalasin D at concentrations within the range 1–20 μg ml^{-1}, but the rAT-E138K strain was unaffected. Thus, macropinoendocytosis by Vero cells is more important for rAT than for rAT-E138K ($P<0{\cdot}05$; Fig. 5b). Furthermore, nystatin, an inhibitor of caveolae-mediated endocytosis, did not inhibit plaque formation of either the rAT or rAT-E138K strains (Fig. 5c). These results demonstrate that both rAT and rAT-E138K strains predominantly utilize penetration via clathrin-dependent endocytosis, rather than caveolae-mediated endocytosis, in Vero cells. The macropinoendocytosis function may also be involved in penetration of rAT virus, but not in that of rAT-E138K.

Recombinant virus release

Following JEV infection of Vero cells at an m.o.i. of 5 p.f.u. per cell, significantly higher titres of rAT virus were detected in supernatant compared with cell-associated virus at 24–48 h post-inoculation ($P<0{\cdot}05$; Fig. 6a). In contrast, higher titres of rAT-E138K virus were detected consistently in the intracellular fraction than in the supernatant. These significant differences in rAT-E138K virus titres between intra- and extracellular fractions were seen at all time points examined ($P<0{\cdot}05$; Fig. 6b). However, total amounts of replicated rAT virus and rAT-E138K virus were similar (Fig. 6c). These data demonstrate clearly that the point mutation significantly inhibits virus release from infected Vero cells, but does not affect virus replication.

On primary neural cells inoculated with JEV at an m.o.i. of 5 p.f.u. per cell, higher titres of rAT virus were found in supernatant than in cell-associated fractions from 18 h post-inoculation (Fig. 6d). Again, significant differences in rAT virus titres were identified between intra- and extracellular virus titres at 24–72 h post-inoculation ($P<0{\cdot}05$; Fig. 6d). In contrast, higher titres of rAT-E138K virus were also present in the intracellular fraction than in supernatant (Fig. 6e), and significant differences in virus titres were

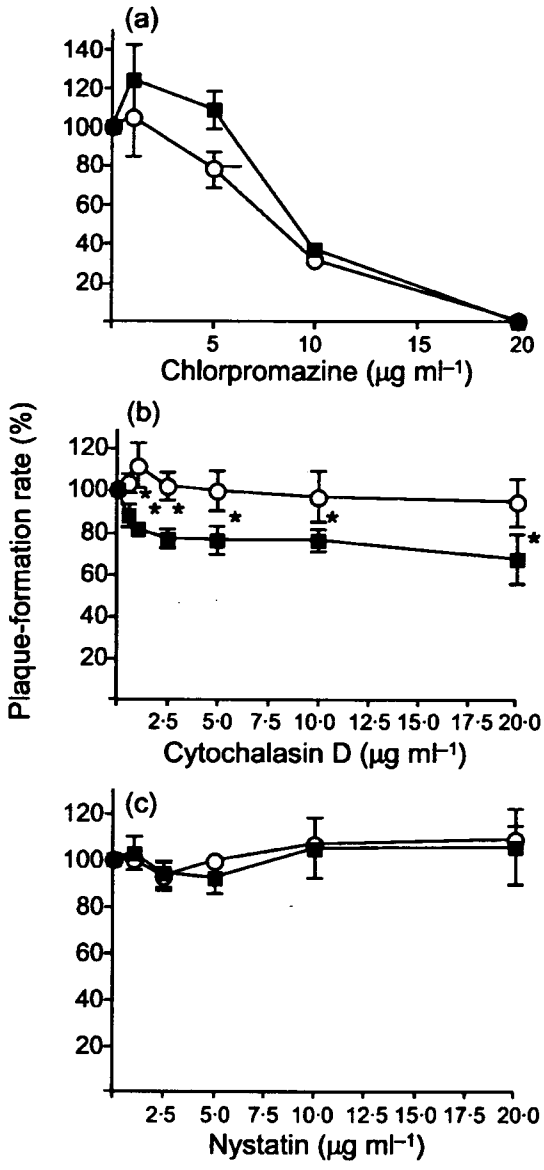

Fig. 5. Inhibition of recombinant JEV internalization on Vero cells. Endocytosis inhibition of rAT (■) and rAT-E138K (○) viruses was examined by using different concentrations of chlorpromazine (a), cytochalasin D (b) and nystatin (c). Each value represents the mean of three separate experiments. Error bars indicate SD. *, $P<0{\cdot}05$.

found between intra- and extracellular fractions at 12–72 h post-inoculation ($P<0{\cdot}05$; Fig. 6e). As with the results for Vero cells, no significant differences in total amounts of replicated virus were observed between rAT and rAT-E138K (Fig. 6f). These results indicate clearly that the point mutation significantly inhibits secretion of replicated virions from both infected Vero cells and primary neural cells.

DISCUSSION

Previous studies have indicated that irregular mutations often taken place at the 5′-end region of full-length JEV cDNA clones (Arroyo *et al.*, 2001; Sumiyoshi *et al.*, 1992; Yun *et al.*, 2003). Through insertion of short introns, the JEV infectious clone was constructed and was able to be propagated stably in *Escherichia coli* (Yamshchikov *et al.*, 2001). In our study, several unforeseen mutations also occurred when the full-length cDNA of AT31 virus was cloned into pBR and pUC vectors (T. Wakita, T. Date, Y. Li & K. Yasui, unpublished data). Focusing on this problem, the 5′-end fragment of JEV AT31 cDNA was cloned into the very low-copy-number pMW118 vector. By inserting another 3′ fragment of JEV, a full-length cDNA of JEV AT31, pMWJEAT, was successfully constructed and amplified. Sequence analysis of viral RNA isolated from the recombinant JEV rAT strain revealed no mutation compared with the template pMWJEAT.

By analogy with three-dimensional structure models of TBE virus (Rey *et al.*, 1995; Mandl *et al.*, 2001) and *Dengue virus* (Zhang *et al.*, 2003b), the E glycoprotein of JEV is predicted to contain an extended structure with seven β-sheets, two α-helices and three domains (Kolaskar & Kulkarni-Kale, 1999). The E glycoprotein is the viral haemagglutinin and induces protective immune responses and mediates receptor-specific viral attachment to cell surfaces. Previous reports have indicated that mutations in the JEV E protein affect viral neurovirulence or neuroinvasiveness *in vivo* (Yu *et al.*, 1981; Ni & Barrett, 1998) or viral binding and entry into cultured cells *in vitro* (Hasegawa *et al.*, 1992; Lee & Lobigs, 2002). The molecular basis of viral attenuation in flaviviruses has been analysed by using site-directed mutagenesis of infectious cDNA clones (Kinney *et al.*, 1997; Hurrelbrink *et al.*, 1999), production of chimeric viruses (Arroyo *et al.*, 2001) and deletions in the 3′ untranslated regions of genomes (Whitehead *et al.*, 2003). Residue 138 of the E protein has been considered to be located on the E0 β-strand in domain I and to be exposed on the surface of the E protein (Lee *et al.*, 2004). The data described in the present manuscript demonstrate that mutation of the E-138 residue in JEV from Glu to Lys inhibits viral spread from cell to cell, explaining the small-plaque morphology. Previous studies have indicated that mutations in domain III of the flavivirus E protein modulate virus binding and entry into host cells (Hung *et al.*, 2004; Liu *et al.*, 2004; Modis *et al.*, 2004). The dimer-to-trimer structural transition of the E protein induced by low-pH conditions is considered crucial for virus–cell binding and entry processes (Stiasny *et al.*, 1996; Chen *et al.*, 1997; Arroyo *et al.*, 2001) and this binding may be affected by mutations in the E protein. The E-138 mutation is not located in domain III, but enhances virus–cell attachment greatly under acidic conditions (Fig. 2).

Flaviviruses are considered to be internalized after binding to glycosaminoglycan (GAG) residues on cells, and other molecules are also involved in virus entry for some viruses

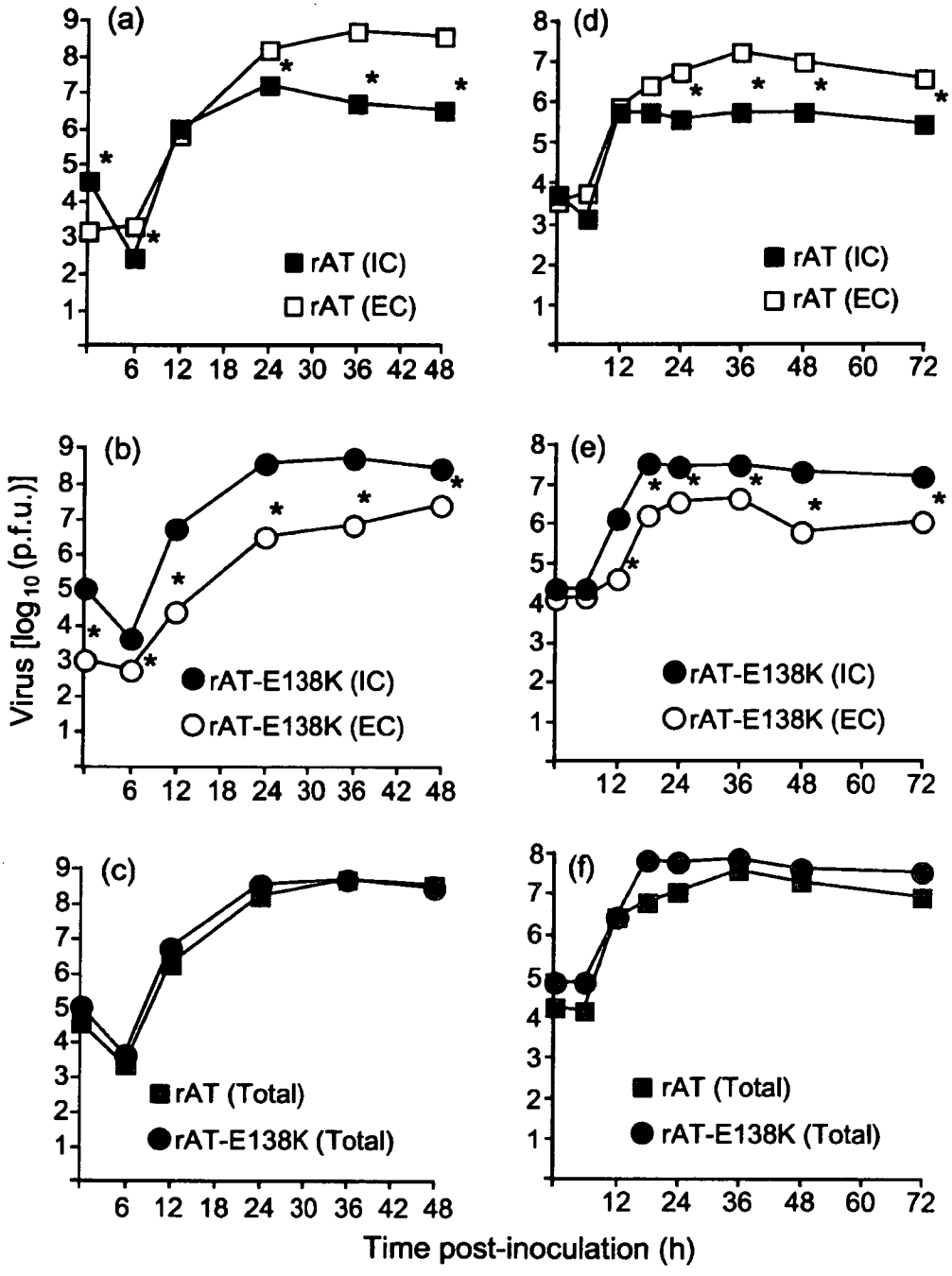

Fig. 6. Replication and secretion of rAT (■, □) and rAT-E138K (●, ○) viruses inoculated into Vero cells. JEV rAT and rAT-E138K strains were inoculated at an m.o.i. of 5 p.f.u. per cell into Vero cells (a–c) or primary neuron cells of BALB/c mice (d–f). Viruses released into the supernatant or retained in the cytoplasm were detected by plaque assay. IC, Intracellular; EC, extracellular; Total, total of intra- and extracellular virus. *, $P<0{\cdot}05$.

(Mandl *et al.*, 2001; Lee *et al.*, 2004; Liu *et al.*, 2004). The binding reaction can be inhibited *in vitro* by using heparin (Chen *et al.*, 1997; Hurrelbrink & McMinn, 2001; Lee & Lobigs, 2002). However, the molecular effects of heparin on virus-binding activity with JEV attenuation are not well understood. Previous studies have indicated that mutations of residues E-49, E-138, E-306 or E-389 on the JEV E protein reduce the efficiency of viral binding to heparan sulphate

residues on target cells (Lee *et al.*, 2004; Liu *et al.*, 2004). Furthermore, cell-adapted TBE virus infection of BHK-21 cells is inhibited by GAGs, whereas this is not the case for the parental virus (Mandl *et al.*, 2001). Mutation at residue E-138 in both JEV and *West Nile virus* shows clearly that this residue is a strong determinant of viral binding to GAG residues on target cells (see Supplementary Table S2, available in JGV Online). In our study, binding by rAT-E138K was inhibited significantly by heparin, whereas the rAT strain was unaffected. Cells digested with heparinase III displayed specifically reduced binding activity to rAT-E138K (Fig. 3). This indicates that rAT-E138K virus binding to cell surfaces is more dependent on heparan sulphate B residues than rAT virus. The better interaction of heparin with rAT-E138K virus in comparison with rAT virus is explained by the fact that heparin is negatively charged and the substitution of negatively charged Glu for positively charged Lys provides a more highly charge-mediated interaction, based on the consideration that residue 138 of the E protein is exposed on the surface (Lee *et al.*, 2004); alternatively, this mutation may expose other positively charged residues on the surface of the virion. Residue E-138 is negatively charged and conserved among the JEV serocomplex, but not among other flaviviruses (See Supplementary Fig. S2, available in JGV Online). Furthermore, a Glu-to-Lys mutation was found not only in JEV, but also in *West Nile virus*. Taken together, the E-138 residue is suggested to be an important determinant of GAG binding and virulence of the JEV serocomplex.

Flaviviruses generally bud into the lumen of the endoplasmic reticulum in infected cells and are subsequently secreted through the vesicle-transport pathway. A recent study has indicated that a single Pro-to-Ser point mutation at position 63 in the prM protein of TBE virus may induce a reduction in virus-particle secretion from RNA-transfected BHK-21 cells (Yoshii *et al.*, 2004). Interestingly, the Glu-to-Lys mutation at E-138 also affects the efficiency of viral release from infected cells. Changes in not only infection efficiency, but also viral secretion efficiency, may play important roles in virus attenuation. Some studies have reported that about 180 glycoprotein E monomers are present on the surface of a mature flavivirus particle with the (pre)M–E heterodimer (Lescar *et al.*, 2001; Kuhn *et al.*, 2002; Zhang *et al.*, 2003a, b). The Glu-to-Lys mutation changes the charge of the side chain from negative to positive. About 180 positively charged side chains at E-138 residues would change to 180 negative charges in each rAT-E138K virus particle. Clearly, this would affect both the binding of rAT-E138K virus to target cells and intracellular transport of viral particles. Furthermore, the E-138 residue exists near the hinge region between domains I and II, and the three-dimensional structure of the E protein might therefore change due to mutation of this residue. Taken together, these mechanisms may attenuate JEV virulence cooperatively *in vivo*, but further study is needed to clarify this point.

Neuroinvasiveness of both at222 and rAT-E138K viruses was attenuated (Table 1). The blood–brain barrier (BBB) can inhibit viral invasion into mouse brains, and both rAT-E138K and at222 viruses proved unable to enter the brain. A recent publication demonstrated that *West Nile virus* replication in peripheral tissues triggers a Toll-like receptor inflammatory response that alters the permeability of the BBB (Wang *et al.*, 2004). Increased BBB permeability allows *West Nile virus* to cross the BBB. *West Nile virus* is a flavivirus that is genetically related very closely to JEV. Similar mechanisms might thus be important for the neuroinvasiveness of JEV. The data in Table 2 demonstrate clearly that rAT-E138K virus does not cause viraemia and, thus, inflammatory responses might be insufficient to replace BBB permeability. This issue warrants further analysis in future.

Previous investigators of the JEV SA14-14-2 strain have demonstrated that change of residue E-279 from methionine to lysine in domain II affects viral neurovirulence significantly (Monath *et al.*, 2002). Our studies indicate that residue E-138, which is located at the link region between domains I and II, is an important determinant of neurovirulence and neuroinvasivenes in JEV. However, the at222 virus contains additional mutations besides E-138 and demonstrated characteristics of further attenuation, compared with rAT-E138K with the single mutation at E-138. The function of point mutations at other residues in the JEV E protein should thus be examined by using full-length cDNA clones in future studies.

ACKNOWLEDGEMENTS

We are grateful to Dr J. Nakamura of the Nippon Institute for Biological Science, Japan, for providing the JEV AT31 strain. We also wish to thank Dr Satoshi Koike for his helpful advice. This work was supported in part by a Grant-in-Aid for Scientific Research from the Japan Society for the Promotion of Science, by a Grant from Toray Industries, Inc., by the Program for Promotion of Fundamental Studies in Health Sciences of the Pharmaceuticals and Medical Devices Agency (PMDA) and by the Research on Health Sciences focusing on Drug Innovation from the Japan Health Sciences Foundation.

REFERENCES

Aihara, S., Rao, C. M., Yu, Y. X., Lee, T., Watanabe, K., Komiya, T., Sumiyoshi, H., Hashimoto, H. & Nomoto, A. (1991). Identification of mutations that occurred on the genome of Japanese encephalitis virus during the attenuation process. *Virus Genes* 5, 95–109.

Allison, S. L., Schalich, J., Stiasny, K., Mandl, C. W., Kunz, C. & Heinz, F. X. (1995). Oligomeric rearrangement of tick-borne encephalitis virus envelope proteins induced by an acidic pH. *J Virol* 69, 695–700.

Arroyo, J., Guirakhoo, F., Fenner, S., Zhang, Z.-X., Monath, T. P. & Chambers, T. J. (2001). Molecular basis for attenuation of neurovirulence of a yellow fever virus/Japanese encephalitis virus chimera vaccine (ChimeriVax-JE). *J Virol* 75, 934–942.

Chen, L.-K., Lin, Y.-L., Liao, C.-L., Lin, C.-G., Huang, Y.-L., Yeh, C.-T., Lai, S.-C., Jan, J.-T. & Chin, C. (1996). Generation and

characterization of organ-tropism mutants of Japanese encephalitis virus *in vivo* and *in vitro*. *Virology* **223**, 79–88.

Chen, Y., Maguire, T., Hileman, R. E., Fromm, J. R., Esko, J. D., Linhardt, R. J. & Marks, R. M. (1997). Dengue virus infectivity depends on envelope protein binding to target cell heparan sulfate. *Nat Med* **3**, 866–871.

Gritsun, T. S. & Gould, E. A. (1998). Development and analysis of a tick-borne encephalitis virus infectious clone using a novel and rapid strategy. *J Virol Methods* **76**, 109–120.

Gualano, R. C., Pryor, M. J., Cauchi, M. R., Wright, P. J. & Davidson, A. D. (1998). Identification of a major determinant of mouse neurovirulence of dengue virus type 2 using stably cloned genomic-length cDNA. *J Gen Virol* **79**, 437–446.

Hasegawa, H., Yoshida, M., Shiosaka, T., Fujita, S. & Kobayashi, Y. (1992). Mutations in the envelope protein of Japanese encephalitis virus affect entry into cultured cells and virulence in mice. *Virology* **191**, 158–165.

Hayasaka, D., Gritsun, T. S., Yoshii, K. & 7 other authors (2004). Amino acid changes responsible for attenuation of virus neurovirulence in an infectious cDNA clone of the Oshima strain of *Tick-borne encephalitis virus*. *J Gen Virol* **85**, 1007–1018.

Heinz, F. X. (1986). Epitope mapping of flavivirus glycoproteins. *Adv Virus Res* **31**, 103–168.

Hung, S.-L., Lee, P.-L., Chen, H.-W., Chen, L.-K., Kao, C.-L. & King, C.-C. (1999). Analysis of the steps involved in dengue virus entry into host cells. *Virology* **257**, 156–167.

Hung, J.-J., Hsieh, M.-T., Young, M.-J., Kao, C.-L., King, C.-C. & Chang, W. (2004). An external loop region of domain III of dengue virus type 2 envelope protein is involved in serotype-specific binding to mosquito but not mammalian cells. *J Virol* **78**, 378–388.

Hurrelbrink, R. J. & McMinn, P. C. (2001). Attenuation of Murray Valley encephalitis virus by site-directed mutagenesis of the hinge and putative receptor-binding regions of the envelope protein. *J Virol* **75**, 7692–7702.

Hurrelbrink, R. J., Nestorowicz, A. & McMinn, P. C. (1999). Characterization of infectious Murray Valley encephalitis virus derived from a stably cloned genome-length cDNA. *J Gen Virol* **80**, 3115–3125.

Kato, T., Miyamoto, M., Furusaka, A., Date, T., Yasui, K., Kato, J., Matsushima, S., Komatsu, T. & Wakita, T. (2003a). Processing of hepatitis C virus core protein is regulated by its C-terminal sequence. *J Med Virol* **69**, 357–366.

Kato, T., Date, T., Miyamoto, M., Furusaka, A., Tokushige, K., Mizokami, M. & Wakita, T. (2003b). Efficient replication of the genotype 2a hepatitis C virus subgenomic replicon. *Gastroenterology* **125**, 1808–1817.

Khromykh, A. A. & Westaway, E. G. (1994). Completion of Kunjin virus RNA sequence and recovery of an infectious RNA transcribed from stably cloned full-length cDNA. *J Virol* **68**, 4580–4588.

Kimura-Kuroda, J. & Yasui, K. (1983). Topographical analysis of antigenic determinants on envelope glycoprotein V3 (E) of Japanese encephalitis virus, using monoclonal antibodies. *J Virol* **45**, 124–132.

Kimura-Kuroda, J., Ichikawa, M., Ogata, A., Nagashima, K. & Yasui, K. (1993). Specific tropism of Japanese encephalitis virus for developing neurons in primary rat brain culture. *Arch Virol* **130**, 477–484.

Kinney, R. M., Butrapet, S., Chang, G.-J. J., Tsuchiya, K. R., Roehrig, J. T., Bhamarapravati, N. & Gubler, D. J. (1997). Construction of infectious cDNA clones for dengue 2 virus: strain 16681 and its attenuated vaccine derivative, strain PDK-53. *Virology* **230**, 300–308.

Kolaskar, A. S. & Kulkarni-Kale, U. (1999). Prediction of three-dimensional structure and mapping of conformational epitopes of envelope glycoprotein of Japanese encephalitis virus. *Virology* **261**, 31–42.

Kuhn, R. J., Zhang, W., Rossmann, M. G. & 9 other authors (2002). Structure of dengue virus: implications for flavivirus organization, maturation, and fusion. *Cell* **108**, 717–725.

Lai, C.-J., Zhao, B., Hori, H. & Bray, M. (1991). Infectious RNA transcribed from stably cloned full-length cDNA of dengue type 4 virus. *Proc Natl Acad Sci U S A* **88**, 5139–5143.

Lee, E. & Lobigs, M. (2002). Mechanism of virulence attenuation of glycosaminoglycan-binding variants of Japanese encephalitis virus and Murray Valley encephalitis virus. *J Virol* **76**, 4901–4911.

Lee, E., Hall, R. A. & Lobigs, M. (2004). Common E protein determinants for attenuation of glycosaminoglycan-binding variants of Japanese encephalitis and West Nile viruses. *J Virol* **78**, 8271–8280.

Lescar, J., Roussel, A., Wien, M. W., Navaza, J., Fuller, S. D., Wengler, G., Wengler, G. & Rey, F. A. (2001). The fusion glycoprotein shell of Semliki Forest virus: an icosahedral assembly primed for fusogenic activation at endosomal pH. *Cell* **105**, 137–148.

Liu, H., Chiou, S.-S. & Chen, W.-J. (2004). Differential binding efficiency between the envelope protein of Japanese encephalitis virus variants and heparan sulfate on the cell surface. *J Med Virol* **72**, 618–624.

Mandl, C. W., Guirakhoo, F., Holzmann, H., Heinz, F. X. & Kunz, C. (1989). Antigenic structure of the flavivirus envelope protein E at the molecular level, using tick-borne encephalitis virus as a model. *J Virol* **63**, 564–571.

Mandl, C. W., Kroschewski, H., Allison, S. L., Kofler, R., Holzmann, H., Meixner, T. & Heinz, F. X. (2001). Adaptation of tick-borne encephalitis virus to BHK-21 cells results in the formation of multiple heparan sulfate binding sites in the envelope protein and attenuation in vivo. *J Virol* **75**, 5627–5637.

Modis, Y., Ogata, S., Clements, D. & Harrison, S. C. (2004). Structure of the dengue virus envelope protein after membrane fusion. *Nature* **427**, 313–319.

Monath, T. P. & Heinz, F. X. (1996). Flaviviruses. In *Fields Virology*, 3rd edn, pp. 961–1034. Edited by B. N. Fields, D. M. Knipe & P. M. Howley. Philadelphia, PA: Lippincott-Raven.

Monath, T. P., Arroyo, J., Levenbook, I., Zhang, Z.-X., Catalan, J., Draper, K. & Guirakhoo, F. (2002). Single mutation in the flavivirus envelope protein hinge region increases neurovirulence for mice and monkeys but decreases viscerotropism for monkeys: relevance to development and safety testing of live, attenuated vaccines. *J Virol* **76**, 1932–1943.

Ni, H. & Barrett, A. D. T. (1998). Attenuation of Japanese encephalitis virus by selection of its mouse brain membrane receptor preparation escape variants. *Virology* **241**, 30–36.

Nitayaphan, S., Grant, J. A., Chang, G.-J. J. & Trent, D. W. (1990). Nucleotide sequence of the virulent SA-14 strain of Japanese encephalitis virus and its attenuated vaccine derivative, SA-14-14-2. *Virology* **177**, 541–552.

Polo, S., Ketner, G., Levis, R. & Falgout, B. (1997). Infectious RNA transcripts from full-length dengue virus type 2 cDNA clones made in yeast. *J Virol* **71**, 5366–5374.

Reed, L. J. & Muench, H. (1938). A simple method of estimating fifty percent endpoints. *Am J Hyg* **27**, 493–497.

Rey, F. A., Heinz, F. X., Mandl, C., Kunz, C. & Harrison, S. C. (1995). The envelope glycoprotein from tick-borne encephalitis virus at 2 Å resolution. *Nature* **375**, 291–298.

Rice, C. M., Grakoui, A., Galler, R. & Chambers, T. J. (1989). Transcription of infectious yellow fever virus RNA from full-length cDNA templates produced by in vitro ligation. *New Biol* **1**, 285–296.

Shi, P.-Y., Tilgner, M., Lo, M. K., Kent, K. A. & Bernard, K. A. (2002). Infectious cDNA clone of the epidemic West Nile virus from New York City. *J Virol* **76**, 5847–5856.

Stiasny, K., Allison, S. L., Marchler-Bauer, A., Kunz, C. & Heinz, F. X. (1996). Structural requirements for low-pH-induced rearrangements in the envelope glycoprotein of tick-borne encephalitis virus. *J Virol* **70**, 8142–8147.

Stiasny, K., Allison, S. L., Schalich, J. & Heinz, F. X. (2002). Membrane interactions of the tick-borne encephalitis virus fusion protein E at low pH. *J Virol* **76**, 3784–3790.

Sumiyoshi, H., Mori, C., Fuke, I., Morita, K., Kuhara, S., Kondou, J., Kikuchi, Y., Nagamatu, H. & Igarashi, A. (1987). Complete nucleotide sequence of the Japanese encephalitis virus genome RNA. *Virology* **161**, 497–510.

Sumiyoshi, H., Hoke, C. H. & Trent, D. W. (1992). Infectious Japanese encephalitis virus RNA can be synthesized from in vitro-ligated cDNA templates. *J Virol* **66**, 5425–5431.

Sumiyoshi, H., Tignor, G. H. & Shope, R. E. (1995). Characterization of a highly attenuated Japanese encephalitis virus generated from molecularly cloned cDNA. *J Infect Dis* **171**, 1144–1151.

Wang, T., Town, T., Alexopoulou, L., Anderson, J. F., Fikrig, E. & Flavell, R. A. (2004). Toll-like receptor 3 mediates West Nile virus entry into the brain causing lethal encephalitis. *Nat Med* **10**, 1366–1373.

Whitehead, S. S., Falgout, B., Hanley, K. A., Blaney, J. E., Jr, Markoff, L. & Murphy, B. R. (2003). A live, attenuated dengue virus type 1 vaccine candidate with a 30-nucleotide deletion in the 3′ untranslated region is highly attenuated and immunogenic in monkeys. *J Virol* **77**, 1653–1657.

Wilcox, C. L., Smith, R. L., Freed, C. R. & Johnson, E. M., Jr (1990). Nerve growth factor-dependence of herpes simplex virus latency in peripheral sympathetic and sensory neurons *in vitro*. *J Neurosci* **10**, 1268–1275.

Yamshchikov, V., Mishin, V. & Cominelli, F. (2001). A new strategy in design of (+)RNA virus infectious clones enabling their stable propagation in *E. coli*. *Virology* **281**, 272–280.

Yasui, K. (2002). Neuropathogenesis of Japanese encephalitis virus. *J Neurovirol* **8** (Suppl. 2), 112–114.

Yoshii, K., Konno, A., Goto, A. & 7 other authors (2004). Single point mutation in tick-borne encephalitis virus prM protein induces a reduction of virus particle secretion. *J Gen Virol* **85**, 3049–3058.

Yu, Y. X., Wu, P. F., Ao, J., Liu, L. H. & Li, H. M. (1981). Selection of a better immunogenic and highly attenuated live vaccine virus strain of JE. I. Some biological characteristics of SA14-14-2 mutant. *Chin J Microbiol Immunol* **1**, 77–84.

Yun, S.-I., Kim, S.-Y., Rice, C. M. & Lee, Y.-M. (2003). Development and application of a reverse genetics system for Japanese encephalitis virus. *J Virol* **77**, 6450–6465.

Zhang, W., Chipman, P. R., Corver, J. & 7 other authors (2003a). Visualization of membrane protein domains by cryo-electron microscopy of dengue virus. *Nat Struct Biol* **10**, 907–912.

Zhang, Y., Corver, J., Chipman, P. R. & 7 other authors (2003b). Structures of immature flavivirus particles. *EMBO J* **22**, 2604–2613.

Zhao, Z., Wakita, T. & Yasui, K. (2003). Inoculation of plasmids encoding Japanese encephalitis virus PrM-E proteins with colloidal gold elicits a protective immune response in BALB/c mice. *J Virol* **77**, 4248–4260.

Available online at www.sciencedirect.com
ScienceDirect
Journal of Virological Methods 148 (2008) 174–181
Journal of Virological Methods
www.elsevier.com/locate/jviromet

Dynamic behavior of hepatitis C virus quasispecies in a long-term culture of the three-dimensional radial-flow bioreactor system

Kyoko Murakami[a], Yasushi Inoue[a,b], Su-Su Hmwe[a,c], Kazuhiko Omata[a,d], Tomokatsu Hongo[e], Koji Ishii[a], Sayaka Yoshizaki[a], Hideki Aizaki[a], Tomokazu Matsuura[f], Ikuo Shoji[a], Tatsuo Miyamura[a], Tetsuro Suzuki[a,*]

[a] *Department of Virology II, National Institute of Infectious Diseases, 1-23-1 Toyama, Shinjuku-ku, Tokyo 162-8640, Japan*
[b] *Pulmonary and Critical Care Unit, Mita Hospital, International University of Health and Welfare, Japan*
[c] *Department of Infectious Diseases, Internal Medicine, Graduate School of Medicine, University of Tokyo, Tokyo, Japan*
[d] *Department of Oral and Maxillofacial Surgery, The Nippon Dental University School of Dentistry at Tokyo, Tokyo, Japan*
[e] *ABLE Corporation, Shizuoka, Japan*
[f] *Department of Laboratory medicine, The Jikei University School of Medicine, Tokyo, Japan*

Received 25 July 2007; received in revised form 9 November 2007; accepted 21 November 2007

Abstract

Hepatitis C virus (HCV) exists in infected individuals as quasispecies, usually consisting of a dominant viral isolate and a variable mixture of related, yet genetically distinct, variants. A prior HCV infection system was developed using human hepatocellular carcinoma cells cultured in the three-dimensional radial-flow bioreactor (RFB), in which the cells retain morphological appearance and their differentiated hepatocyte functions for an extended period of time. This report studies the selection and alteration of the viral quasispecies in the RFB system inoculated with pooled serum derived from HCV carriers. Monitoring the viral RNA and core protein in the culture supernatants, together with nucleotide sequencing of hypervariable region 1 of the HCV genome, demonstrated that (1) the virus production intermittently fluctuated in the cultures, (2) the viral genetic diversity was markedly reduced 3 days post-infection (p.i.), and (3) dominant species changed on days 19–33 p.i., suggesting that the virus populations can be selected according to susceptibility to the viral infection and replication. A therapeutic effect of interferon-α also demonstrated the inhibition of HCV expression. Thus, this HCV infection model in the RFB system should be useful for investigating the dynamic behavior of HCV quasispecies in cultured cells and evaluating anti-HCV compounds.

Keywords: Hepatitis C virus; Three-dimensional culture; Radial-flow bioreactor; Dynamics; Quasispecies

1. Introduction

Hepatitis C virus (HCV) is a major cause of chronic liver diseases (Choo et al., 1989; Kuo et al., 1989; Saito et al., 1990) and has been estimated to infect more than 170 million people throughout the world (Poynard et al., 2003). Symptoms of persistent HCV infection extend from chronic hepatitis to cirrhosis and ultimately hepatocellular carcinoma (Choo et al., 1989; Kuo et al., 1989; Saito et al., 1990). HCV belongs to the genus *Hepacivirus*, included in the family of Flaviviridae, and possesses a viral genome of a single, positive-stranded RNA with a nucleotide (nt) length of approximately 9.6 kb (Choo et al., 1991; Grakoui et al., 1993; Hijikata et al., 1991). It has been shown that HCV, like many other RNA viruses, circulates within infected individuals as a diverse population and closely related variants are referred to as quasispecies (Martell et al., 1992). This quasispecies model of mixed virus populations may imply a significant survival advantage because the simultaneous presence of multiple variant genomes and/or high rate of generation of new variants allow rapid selection of the mutants are better suited to new environmental conditions (Pawlotsky, 2006).

Studies on HCV replication and development of selective antiviral drugs have been hampered primarily by the lack of efficient cell culture systems. Establishment of selectable dicistronic HCV RNAs that are capable of autonomous replication to high levels in human hepatoma Huh-7 cells was a

* Corresponding author. Tel.: +81 3 5285 1111; fax: +81 3 5285 1161.
E-mail address: tesuzuki@nih.go.jp (T. Suzuki).

0166-0934/$ – see front matter © 2007 Elsevier B.V. All rights reserved.
doi:10.1016/j.jviromet.2007.11.001

significant breakthrough in HCV research; however, virus production has not been observed in the conventional monolayer cultures (Blight et al., 2000; Lohmann et al., 1999). Recently, it has been described that infectious HCV particles are efficiently produced from a genotype 2a isolate JFH-1 in Huh-7 cells (Blight et al., 2000; Wakita et al., 2005; Zhong et al., 2005). This JFH-1 based HCV culture system is an invaluable achievement permitting a variety of studies on the complete HCV life cycle. However, HCV infection systems with human sera or plasmas containing intact virions are still limited because of low levels of propagation in the cultures. Reverse transcription (RT)-PCR was typically used to detect the viral RNA in cell extracts; however, synthesized viral proteins were not observed in these systems (Ikeda et al., 1998; Tagawa et al., 1995).

There are reports of differentiated human hepatoma FLC4 (functional liver cell 4) cells grown in a three-dimensional (3D) radial-flow bioreactor (RFB) that can be infected by HCV-positive serum and support viral replication (Aizaki et al., 2003). Furthermore, production and release of infectious HCV has been observed in the RFB system following transfection of FLC4 cells with *in vitro* transcribed HCV genomic RNA, as well as in a 3D system using Huh-7 cells harboring genome-length dicistronic RNAs (Murakami et al., 2006). The RFB system, in which the bioreactor column consists of a cylindrical matrix with porous bead microcarriers extended vertically, was aimed initially at developing artificial liver tissues and allows liver-derived cells to maintain morphological appearance as well as their physiological functions, such as the ability to synthesize albumin and drug-metabolizing activity mediated by cytochrome P450 (Iwahori et al., 2003). The radial-flow configuration permits full contact between culture medium and cells at a physiologic perfusion flow rate, and prevents excessive shear stresses and buildup of waste products, thus ensuring the long-term viability of 3D cell culture.

The aim of the present study was to characterize HCV dynamics in the RFB system during long-term cultures inoculated with pooled serum obtained from HCV carriers, and to examine the therapeutic effects of interferon-alpha (IFN-α) in this HCV infection model.

2. Materials and methods

2.1. Cell cultures

FLC4 cells (Aoki et al., 1998), which were derived from human hepatocellular carcinoma cells and negative for HCV RNA and HBV DNA, were maintained in serum-free ASF104 medium (Ajinomoto, Japan) supplemented with 4 g/L D-glucose on the collagen-coated dishes before inoculating into the RFB column. The RFB system (ABLE, Japan) was manipulated as described previously (Aizaki et al., 2003) with minor modifications. Briefly, RFB columns, which have bed volumes of 30 or 4 mL and are filled with porous glass microcarriers (diameter 0.6 mm, vacant capacity 50%, pore size <120 μm) (Hongo et al., 2005), were seeded with FLC4 cells, which subsequently attached to the surface and inside of porous glass beads. ASF104 medium containing 2% fetal calf serum was added at a flow rate of 50 mL/day, and the culture condition was automatically controlled by monitoring temperature, pH value and oxygen levels in the vessel throughout the duration of the study.

2.2. Infection of HCV-positive sera

HCV antibody-positive sera used in this study were blood donor samples supplied by The Japanese Red Cross Center, Tokyo, Japan. HCV RNA loads in the sera were as follows: serum A, 2.4×10^6 copies/mL; serum B, 8.6×10^6 copies/mL; serum C, 5.9×10^6 copies/mL; serum D, 2.5×10^6 copies/mL; serum E, 1.0×10^7 copies/mL; serum F, 1.4×10^7 copies/mL (Table 1). In the first experiment (Fig. 3), aliquots of each serum containing 2×10^6 copies of HCV RNA were mixed and pooled serum sample with 1.2×10^7 copies was prepared as an inoculum. The pooled serum (2.5 mL) was added to the 3D cultured-FLC4 cells in the 30-mL RFB column, and the culture medium was changed after 12 h of incubation. At various times during the culture period, culture medium (50 mL) was collected to determine HCV RNA and the core protein. Collected culture media were passed through a 0.20-μm filter to remove the debris, and stored at −80 °C. In the second experiment to evaluate a therapeutic effect of anti-HCV drug (Fig. 4), 4-mL RFB columns were used. IFN-α (Sumiferon 300; Sumitomo Pharmaceuticals, Japan) was added to one of two columns at a final concentration of 100 IU/mL after the infection. Culture medium was periodically collected for determination of HCV RNA, the core protein and transaminases, and was replaced with the same volume of fresh medium with or without IFN-α.

2.3. Quantitation of HCV RNA and core protein

HCV RNA was extracted from 140 μL of each serum or culture medium using QIAamp Viral RNA Mini spin column (QIAGEN); RNA was eluted in 60 μL of water and stored at −80 °C. Real-time RT-PCR was performed using TaqMan EZ RT-PCR Core Reagents (PE Applied Biosystems), as described previously (Aizaki et al., 2003; Suzuki et al., 2005). The viral core antigen in the culture medium was quantified by immunoassay (Ortho HCV-Core ELISA Kit; Ortho-Clinical Diagnotics), according to the manufacturer's instruction (Murakami et al., 2006).

2.4. PCR amplification and nucleotide sequencing of HVR1 domain and its flanking region

Five microliters of RNA samples prepared as above were reverse transcribed using SuperScript II (Invitrogen) and a specific primer 5′-CATCCATGTGCAGCCGAACC-3′ (corresponding to nucleotides [nt] 2006–1987 of HCV NIHJ1) (Aizaki et al., 1998). For the nested PCR, a genotype-independent set of primers specific for hypervariable region 1 (HVR1). The first round of PCR was performed with the outer sense primer 5′-GCATGGCTTGGGATATGATG-3′ (nt 1291–1310) and with the reverse transcription primer described above as the outer antisense primer. After the initial 3.5-min denaturation step at 94 °C, 35 PCR cycles, with each cycle

Table 1
HCV-positive sera used in this study

Serum	Clone	HCV HVR1 sequence	% in the serum	genotype
A	A1	KVLIVMLSFAGVDGSTRTIGGRTAHTTQGSASLFSSGPAQKIQLINTNGS	75	1
	A2	-------L------N-H-V--AV-SS---FT---KL----------S---	12.5	
	A3	-------L------N-YAS---AGLL-R-V--I-TA----------S---	12.5	
B	B1	KVVVILLLAAGVDAGTNTIGGSAAQTTSGFTGLFRSGARQNIQLINTNGS	50	2
	B2	----------R	12.5	
	B3	----------S---------	12.5	
	B4	--L-V---F-----E-HVT--N-GR--A-LV--LTP--K----------	12.5	
	B5	--I----------	12.5	
C	C1	KVLIVMLLFAGVDGDTHVSGGTQGRAAYGLASLFALGPTQKIQLVNTNGS	83.3	1
	C2	----------A----------	16.7	
D	D1	KVLIVMLLFAGVDGVTHTSGAAAGHNARSLSGLFSLGSAQKLQLINTNGS	40	1
	D2	----------A-Y---GT--Y-TKTFT-F--R-PS--I--------	20	
	D3	----------T--Y---T-T----P--------V-----	10	
	D4	----------V---T----P--------V-----	10	
	D5	----------V-----	10	
	D6	----------Y-T--FT----S-----I--V-----	10	
E	E1	KVLIVMLLFAGVDGSTRVSGGQAGRVTKSLASFFSPGPQQKIQLVNSNGS	40	1
	E2	----------HGFT-L--A-S----------	30	
	E3	----------QGFT-L--A-S----------	10	
	E4	----------S-FT-L-TV----------	10	
	E5	----------N-Y---------AH--T-L--A-S----------	10	
F	F1	KVLIVMLLFAGVDGETNVMGGRAGHTTNTFTSLFSVGPAQKIQLVNSNGS	37	1
	F2	----------D-K----------S-L----N---S----------	27	
	F3	----------K----Q-----S-L----N---S----------	18	
	F4	----------A-------A--TK---------D----	9	
	F5	----------G--------A--A--L----TR--S----------	9	

consisting of 1 min at 94 °C, 2 min at 45 °C, and 3 min at 72 °C, were carried out, followed by a 10-min extension step at 72 °C. The second round was performed with the inner sense primer 5′-GGTAAGCTTTCCATGGTGGGGAACTGGGC-3′ (nt 1419–1447) and the inner antisense primer 5′-CTGGAATTCGCAGTCCTGTTGATGTGCCA-3′ (nt 1627–1599). The amplified products were cloned into the pGEM-T vector (Promega), and at least 8 independent clones were sequenced with an automatic DNA sequencer (ABI PRISM 310, PE Applied Biosystems).

3. Results

3.1. The outline of the RFB system

The RFB system was initially aimed at developing artificial liver tissues and allows liver-derived cells to maintain morphological appearance as well as their physiological functions, such as the ability to synthesize albumin and drug-metabolizing activity mediated by cytochrome P450 (Iwahori et al., 2003). Fig. 1 shows the outline of the RFB system. The bioreactor column consists of a vertically extended cylindrical matrix with porous glass microcarriers, which were most suitable for FLC4 culture as described in Section 2. The conditioning vessel is connected to a circulation system including tanks either for supplying fresh medium or for recovering sample aliquots. Oxygen consumption, temperature and pH of the culture medium are monitored continuously and conditioned in the vessel by computer and mass flow controller throughout the culture. Thus, the radial-flow configuration permits full contact between culture medium and cells at a physiologic perfusion flow rate, and prevents excessive shear stresses and a buildup of waste products, thus ensuring the long-term viability of 3D culture. For the long-term culture up to 110 days, temperature in the vessel gradually decreased from 37 to 30 °C as shown in Fig. 2A. The oxygen consumption, which indicates the cell growth condition, increased slowly from days 0 to 80 post-inoculation of the cells, and maintained a constant level afterwards. Under this condition, the production rate of albumin was found to be stable from days 15 to 105. The following experiments of HCV infection were done in such a stable phase of the cell condition after 3 weeks of pre-culture. Cell grown in the RFB column reached confluence at the end of culture (day 110) since the cells were observed outside the matrix bed (Fig. 2B).

3.2. Infection of HCV-positive sera to RFB cultured FLC4 cells

Previously, HCV RNA could be detected in FLC4 cells grown in the RFB up to 4 weeks of culture following inoculation with an HCV carrier plasmid (Aizaki et al., 2003). Establishment of a long-term stable culture system of human liver-derived cells

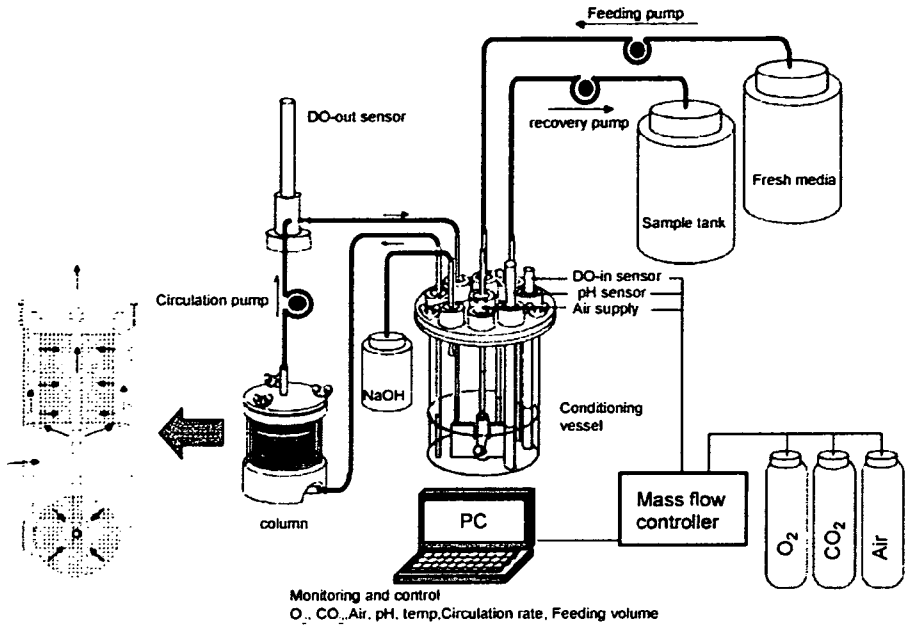

Fig. 1. Outline of the RFB system. RFB system consists of vessel, column and PC monitoring system. Culture condition was automatically controlled: oxgen concentration, temperature, pH, and oxgen level in the conditioning vessel are continuously monitored by PC and conditioned by mass flow controller.

retaining their differentiated hepatocyte function, as described above, enables evaluations of dynamic analysis of HCV replication and selection of viral variability and quasispecies. The potential of this culture system for screening HCV-positive sera was well suited for the viral infection.

Table 1 shows the serum samples (A–F) from six HCV carriers. The nucleotide complexity of HCV in serum samples was determined by sequencing the 1449–1598 nt region of the HCV genome, which includes HVR1 located at the N-terminal region of E2. Each serum was a mixture of a dominant HCV clone and related but distinct viral populations. The dominant species in sera A, C, D, E, and F were found to be genotype 1, and that in serum B was genotype 2. Viral loads in A–F, respectively, were 2.4×10^6, 8.6×10^6, 5.9×10^6, 2.5×10^6, 1.0×10^7 and 1.4×10^7 copies/mL, which were determined by real-time RT-PCR, as previously described (Aizaki et al., 2003; Suzuki et al., 2005). HCV loads of 2×10^6 copies from each serum sample were mixed to prepare a pooled serum sample containing 1.2×10^7 copies of HCV RNA. After FLC4 cells were inoculated into the RFB and subjected to 2 weeks of pre-culture for the preparation of 3D culture, the cells were infected with the pooled serum. Cell number at infection was about 10^8 in the 30-

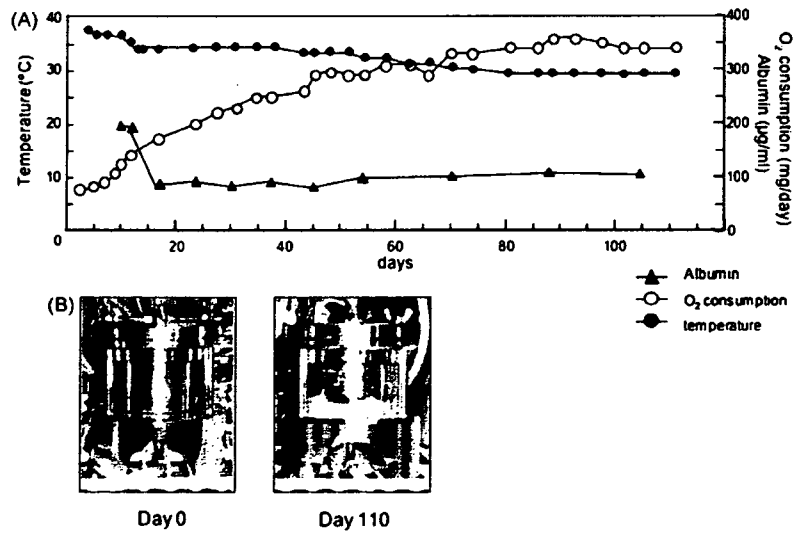

Fig. 2. Long-term culture of FLC4 cells in the RFB system. (A) Long-term culture of FLC4 cells in the RFB system. Temperature (closed circles) was gradually decreased from 37 to 30 °C. Oxygen consumption (open circles) was gradually increased from days 0 to 80 and reached the steady-state level. Albumin concentration (closed triangles) was constant from days 15 to 105. (B) The appearance of the RFB column at the beginning (day 0) and at the end (day 110) of culture.

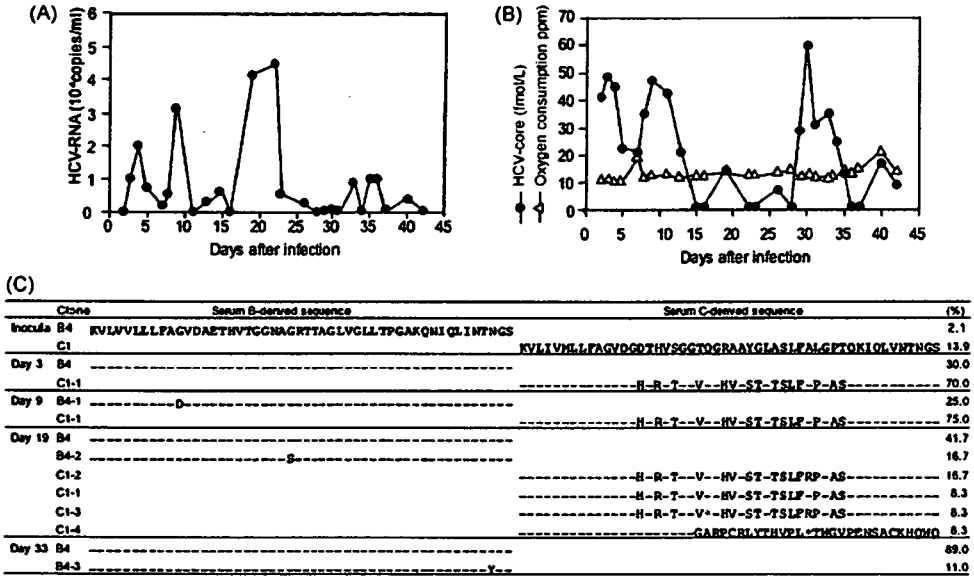

Fig. 3. HCV propagation in FLC4 cells cultured in the RFB system following inoculation with pooled sera obtained from HCV carriers. The 3D-cultured FLC4 cells were incubated with a pooled serum sample for 12 h, followed by changing the culture medium to fresh one. Culture medium was periodically collected for 42 days after inoculation, and HCV RNA and the viral core protein were quantified, respectively, by real-time RT-PCR and ELISA. (A) HCV RNA level in culture supernatant. (B) HCV-core protein (closed circles) and oxygen consumption (open triangles) levels in culture supernatant. (C) Changes in the viral quasispecies distribution after the inoculation. Percentages in the inoculum or in the culture medium at each time point (day 3, 9, 19, or 33 p.i.) are indicated at the right side. *, termination codon.

mL RFB column, as estimated from the glucose consumption (Kawada et al., 1998). Culture medium in the RFB was replaced with fresh medium 12 h post-infection (p.i.) and periodically sampled for 42 days.

Fig. 3A and B shows the levels of HCV RNA and viral core protein in the culture medium, respectively. HCV RNA was not observed on the first 2 days following infection, but was detectable from day 3 p.i. Viral RNA levels fluctuated, with peaks on days 3, 9, 19–21 and 33–36 p.i. At days 19–21 p.i., the average amount of HCV RNA detected in the culture supernatant was approximately 3×10^6 copies/day. Intermittent peaks were observed in HCV core protein levels in the culture supernatant, and the peak pattern of the core protein was largely consistent with that of viral RNA. During the infection experiment, the level of oxygen consumption was constant at approximately 12 ppm, thus suggesting that the desired conditions (constant or very gradually increasing cell number) were maintained.

3.3. Quasispecies analysis in RFB culture

The above results suggest that, although the environment was consistent in the pooled serum infection, there were periods in which the viruses actively replicated and released from the cells and periods in which they poorly replicated. The pooled serum used for the infection exhibited HCV populations had at least 26 distinct quasispecies (Table 1). To investigate whether the quasispecies distribution was altered due to infection, and whether HCV populations are selected during long-term culture in the RFB, total RNA was extracted from the culture supernatant samples collected on days 3, 9, 19 and 33 p.i., and the nucleotide sequence of the region containing HVR1 was determined, as described above. As shown in Fig. 3C, it is of interest that only two HCV species were detected in the sample at day 3 p.i.; the dominant clone C1-1, comprising approximately 70% of the viral population, and clone B4, comprising 30%. Although clone C1-1 was not detected in the sequence of the inoculum shown in Table 1, it was most similar to clone C1, a dominant clone in plasma C, among the HCV population observed in the inoculum; thus, it is possible that clone C1-1 is one of the minor species in serum C. Clone B4 was found to be derived from serum B. An almost identical HCV population was observed in the sample at day 9 p.i. In this sample, the dominant clone C1-1 and clone B4-1, which differs from clone B4 by only one amino acid, were detected. In contrast, more significant variation in quasispecies structure of the HCV species was observed in the sample at day 19 p.i. than that at day 9 p.i. With B4 as the dominant clone, the serum B-derived HCV species, clones B4 and B4-2, which differs from clone B4 by one amino acid, comprised 58% of the total population. Four types of HCV sequences derived from serum C were detected. Two of these (clones C1-3 and C1-4) contained lethal mutations. It was also found that the HCV species detected in the sample at day 33 p.i. included only two clones (clones B4 and B4-3), derived from serum B. The dominant clone, B4, was found to comprise 89% of the total population.

3.4. Potential use of the RFB system for evaluation of anti-HCV compounds

An experiment was carried out to determine whether this HCV infection experiment system was useful for the evaluation of anti-HCV drugs (Fig. 4). For this purpose, a small,

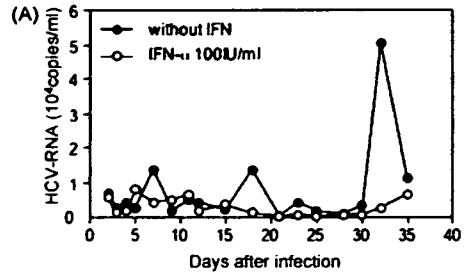

(B)

	Clone		(%)
Inocula	B4	KVLVVLLLFAGVDAETHVTGGSAGRTTAGLVGLLTPGAKQNIQLINTNGS	2.1
	C1	KVLIVTLLFAGVDGDTHVSGGTQGRAAYGLASLFALGFTQKIQLVNTNGS	13.9
Day 32	B4	----------	60
	B4-4	----------*----------	20
	C1-1	----------H-R-T--V--HV-ST-TSLF-P-AS----------	20

Fig. 4. A therapeutic effect of IFN in HCV infection model in the RFB cultures. HCV-infected FLC4 cells were treated with or without 100 IU/mL IFN-α. (A) Culture media were periodically collected, and HCV RNA levels were determined. Closed circles: without IFN treatment, open circles: treatment with IFN. (B) Changes in the viral quasispecies distribution in the cells without IFN treatment. Percentages in the inoculum or in the culture medium on day 32 p.i. are indicated at the right side. *, termination codon.

4-mL RFB column was adopted and a pair of RFB cultures infected with the HCV-positive pooled plasma (Table 1) was prepared. IFN-α was added to one culture at a final concentration of 100 IU/mL at 12 h p.i. No cytotoxicity was observed in FLC4 cells under these conditions (data not shown). Culture media from two cultures (12.5 mL each) were sampled periodically for 35 days and replaced by the same volume of fresh medium in the presence or absence of IFN-α. HCV RNA in the collected media was quantified by real-time RT-PCR, as described above. As shown in Fig. 4A, in the no-treatment culture, fluctuations in the viral RNA levels with the peaks on days 7, 18, and 32 p.i. ($1.5–5 \times 10^4$ copies/mL) were observed. However, while HCV RNA at $0.5–0.8 \times 10^4$ copies/mL was detected in the IFN-treated culture at days 5–11 p.i., no HCV RNA was detected at days 12–30 p.i. Serum levels of hepatic transaminases such as ALT and AST are known to be markers of liver damage. In the HCV-infection model with FLC4 cells cultured in RFB, the AST levels in the culture medium, which ranged from 5 to 10 IU/L without HCV infection, increased to 20–50 IU/L according to the viral infection (data not shown). Such increased AST levels were found to fall by the IFN treatment to lower than 10 IU/L at day 28 p.i. As reported previously, the ALT levels in the culture medium were constantly low; its levels were less than 10 IU/mL, with or without HCV infection (Aizaki et al., 2003). The viral nucleotide sequence in the no-treatment culture medium at day 32 p.i. was determined. It was found that serum B-derived clone B4 was dominant, and serum C-derived clone C1 was present as a minor clone (Fig. 4B); thus, the results corresponded well with those demonstrated in Fig. 3. An increase in viral RNA in the IFN-treated culture after day 32 p.i. was observed; although the degree of increase was only slight (Fig. 4A). It will be interesting to test whether HCV species grown in the IFN-treated culture is a variant resistant to IFN-α.

4. Discussion

At present an important limitation of the *in vitro* HCV infection system is that the only established culture system is based on genotype 2a, JFH-1 isolate, and Huh-7-derived cell lines. The development of alternate infection systems in which other HCV strains and host cells are available has been needed for the study of HCV dynamics and virus–host interactions, and for testing antivirals. This paper demonstrates that a long-term culture of the 3D RFB system is a useful tool for investigating HCV dynamics. The present results revealed that the viral quasispecies distribution altered in the HCV infection system in the RFB system. The change probably occurs in the following two-stage process. The first change was observed on day 3 p.i.; thus, it is possible that the HCV species were selected according to infectivity in FLC4 cells. It has been reported that HCV particle populations in chronic hepatitis C patients consist of low-density virions and higher-density immune complex forms (Hijikata et al., 1993; Kanto et al., 1994). Inoculation of cultured cells with HCV has demonstrated that the immune complex forms were less infective than the antibody-unbound virions (Shimizu et al., 1994). Therefore, another hypothesis may be that a large number of HCV populations in sera A, D, E, and F are immune complex forms; thus, these sera are less susceptible to the cells than sera B and C. The second change was observed on days 19–33 p.i. While the serum C-derived clone was dominant in the early stages after infection, the serum B-derived HCV clone became dominant over time. In the absence of immunological selection pressure, viral nucleotide mutations at random positions are accumulated during viral replication, and the newly generated variant species are selected principally, if not solely, based on the intrinsic replicative advantages or disadvantages that these mutations confer. Thus, these results suggest that the use of pooled serum sample allowed for screening of infectious materials compatible for the RFB culture.

Evaluation methods for anti-HCV drugs using monolayer culture systems with various culture cells, such as the replicon system and the JFH-1 based virion production system, have been reported (Bartenschlager et al., 2003; Blight et al., 2000; Boriskin et al., 2006; Lanford et al., 2003; Lindenbach et al., 2005; Lohmann et al., 1999; Wakita et al., 2005; Zhong et al., 2005). These methods utilize viral markers, such as HCV RNA and antigens, as indicators of treatment efficacy. However, the utility of long-term cell culture systems for anti-HCV drug evaluation based on infection with human sera is still limited. The use of a chimpanzee model, the only non-human host for HCV infection, is restricted due to several reasons such as problematic availability and ethical consideration. Given intensive efforts to reduce and replace animal testing in the course of development of new therapies worldwide, the RFB-based HCV infection model is a potential alternative to animal models such chimpanzee for assessing anti-HCV compounds. According to the studies with regards to mathematical modeling of HCV kinetics (Dahari et al., 2005; Dixit et al., 2004; Layden et al., 2003; Layden-Almer et al., 2006; Perelson et al., 2005), IFN therapy against HCV infection generally generates a biphasic decline in viral load; there is a rapid decrease in the serum HCV RNA level over the

first 1 day of treatment, followed by the second phase, which is slower than the first-phase viral decline. To date, there were no such observable viral kinetics in the IFN treatment under such experimental settings. Further detailed kinetic analyses of the use of varying doses of IFN and of very early time points to evaluate the antiviral effect are in progress.

In summary, by investigating the dynamics of HCV populations in the RFB culture system, it was demonstrated that HCV was intermittently detected in the culture supernatants of long-term culture, and that changes in viral quasispecies appear to be related to this fluctuation in the virus level. It was also shown that an HCV-infection model using the RFB system is useful for evaluating potential antivirals. Further investigation on the infection and growth of various HCV-positive sera is currently being conducted in order to obtain an adaptive clone with higher replication efficiency in this culture system.

Acknowledgements

The authors thank T. Wakita and S. Nagamori for helpful discussion and suggestions. We also thank M. Matsuda, T. Shimoji and M. Yahata for technical assistance, and T. Mizoguchi for secretarial work. This work was supported in part by a grant for Research on Health Sciences focusing on Drug Innovation from the Japan Health Sciences Foundation; by grants-in-aid from the Ministry of Health, Labor and Welfare; and by the program for Promotion of Fundamental Studies in Health Sciences of the National Institute of Biomedical Innovation, Japan.

References

Aizaki, H., Aoki, Y., Harada, T., Ishii, K., Suzuki, T., Nagamori, S., Toda, G., Matsuura, Y., Miyamura, T., 1998. Full-length complementary DNA of hepatitis C virus genome from an infectious blood sample. Hepatology 27, 621–627.

Aizaki, H., Nagamori, S., Matsuda, M., Kawakami, H., Hashimoto, O., Ishiko, H., Kawada, M., Matsuura, T., Hasumura, S., Matsuura, Y., Suzuki, T., Miyamura, T., 2003. Production and release of infectious hepatitis C virus from human liver cell cultures in the three-dimensional radial-flow bioreactor. Virology 314, 16–25.

Aoki, Y., Aizaki, H., Shimoike, T., Tani, H., Ishii, K., Saito, I., Matsuura, Y., Miyamura, T., 1998. A human liver cell line exhibits efficient translation of HCV RNAs produced by a recombinant adenovirus expressing T7 RNA polymerase. Virology 250, 140–150.

Bartenschlager, R., Kaul, A., Sparacio, S., 2003. Replication of the hepatitis C virus in cell culture. Antivir. Res. 60, 91–102.

Blight, K.J., Kolykhalov, A.A., Rice, C.M., 2000. Efficient initiation of HCV RNA replication in cell culture. Science 290, 1972–1974.

Boriskin, Y.S., Pecheur, E.I., Polyak, S.J., 2006. Arbidol: a broad-spectrum antiviral that inhibits acute and chronic HCV infection. Virol. J. 3, 56.

Choo, Q.L., Kuo, G., Weiner, A.J., Overby, L.R., Bradley, D.W., Houghton, M., 1989. Isolation of a cDNA clone derived from a blood-borne non-A, non-B viral hepatitis genome. Science 244, 359–362.

Choo, Q.L., Richman, K.H., Han, J.H., Berger, K., Lee, C., Dong, C., Gallegos, C., Coit, D., Medina-Selby, R., Barr, P.J., et al., 1991. Genetic organization and diversity of the hepatitis C virus. Proc. Natl. Acad. Sci. U.S.A. 88, 2451–2455.

Dahari, H., Major, M., Zhang, X., Mihalik, K., Rice, C.M., Perelson, A.S., Feinstone, S.M., Neumann, A.U., 2005. Mathematical modeling of primary hepatitis C infection: noncytolytic clearance and early blockage of virion production. Gastroenterology 128, 1056–1066.

Dixit, N.M., Layden-Almer, J.E., Layden, T.J., Perelson, A.S., 2004. Modelling how ribavirin improves interferon response rates in hepatitis C virus infection. Nature 432, 922–924.

Grakoui, A., McCourt, D.W., Wychowski, C., Feinstone, S.M., Rice, C.M., 1993. Characterization of the hepatitis C virus-encoded serine proteinase: determination of proteinase-dependent polyprotein cleavage sites. J. Virol. 67, 2832–2843.

Hijikata, M., Kato, N., Ootsuyama, Y., Nakagawa, M., Shimotohno, K., 1991. Gene mapping of the putative structural region of the hepatitis C virus genome by in vitro processing analysis. Proc. Natl. Acad. Sci. U.S.A. 88, 5547–5551.

Hijikata, M., Shimizu, Y.K., Kato, H., Iwamoto, A., Shih, J.W., Alter, H.J., Purcell, R.H., Yoshikura, H., 1993. Equilibrium centrifugation studies of hepatitis C virus: evidence for circulating immune complexes. J. Virol. 67, 1953–1958.

Hongo, T., Kajikawa, M., Ishida, S., Ozawa, S., Ohno, Y., Sawada, J., Umezawa, A., Ishikawa, Y., Kobayashi, T., Honda, H., 2005. Three-dimensional high-density culture of HepG2 cells in a 5-ml radial-flow bioreactor for construction of artificial liver. J. Biosci. Bioeng. 99, 237–244.

Ikeda, M., Sugiyama, K., Mizutani, T., Tanaka, T., Tanaka, K., Sekihara, H., Shimotohno, K., Kato, N., 1998. Human hepatocyte clonal cell lines that support persistent replication of hepatitis C virus. Virus Res. 56, 157–167.

Iwahori, T., Matsuura, T., Maehashi, H., Sugo, K., Saito, M., Hosokawa, M., Chiba, K., Masaki, T., Aizaki, H., Ohkawa, K., Suzuki, T., 2003. CYP3A4 inducible model for in vitro analysis of human drug metabolism using a bioartificial liver. Hepatology 37, 665–673.

Kanto, T., Hayashi, N., Takehara, T., Hagiwara, H., Mita, E., Naito, M., Kasahara, A., Fusamoto, H., Kamada, T., 1994. Buoyant density of hepatitis C virus recovered from infected hosts: two different features in sucrose equilibrium density-gradient centrifugation related to degree of liver inflammation. Hepatology 19, 296–302.

Kawada, M., Nagamori, S., Aizaki, H., Fukaya, K., Niiya, M., Matsuura, T., Sujino, H., Hasumura, S., Yashida, H., Mizutani, S., Ikenaga, H., 1998. Massive culture of human liver cancer cells in a newly developed radial flow bioreactor system: ultrafine structure of functionally enhanced hepatocarcinoma cell lines. In Vitro Cell Dev. Biol. Anim. 34, 109–115.

Kuo, G., Choo, Q.L., Alter, H.J., Gitnick, G.L., Redeker, A.G., Purcell, R.H., Miyamura, T., Dienstag, J.L., Alter, M.J., Stevens, C.E., et al., 1989. An assay for circulating antibodies to a major etiologic virus of human non-A, non-B hepatitis. Science 244, 362–364.

Lanford, R.E., Guerra, B., Lee, H., Averett, D.R., Pfeiffer, B., Chavez, D., Notvall, L., Bigger, C., 2003. Antiviral effect and virus-host interactions in response to alpha interferon, gamma interferon, poly(i)-poly(c), tumor necrosis factor alpha, and ribavirin in hepatitis C virus subgenomic replicons. J. Virol. 77, 1092–1104.

Layden, T.J., Layden, J.E., Ribeiro, R.M., Perelson, A.S., 2003. Mathematical modeling of viral kinetics: a tool to understand and optimize therapy. Clin. Liver Dis. 7, 163–178.

Layden-Almer, J.E., Cotler, S.J., Layden, T.J., 2006. Viral kinetics in the treatment of chronic hepatitis C. J. Viral Hepat. 13, 499–504.

Lindenbach, B.D., Evans, M.J., Syder, A.J., Wolk, B., Tellinghuisen, T.L., Liu, C.C., Maruyama, T., Hynes, R.O., Burton, D.R., McKeating, J.A., Rice, C.M., 2005. Complete replication of hepatitis C virus in cell culture. Science 309, 623–626.

Lohmann, V., Korner, F., Koch, J., Herian, U., Theilmann, L., Bartenschlager, R., 1999. Replication of subgenomic hepatitis C virus RNAs in a hepatoma cell line. Science 285, 110–113.

Martell, M., Esteban, J.I., Quer, J., Genesca, J., Weiner, A., Esteban, R., Guardia, J., Gomez, J., 1992. Hepatitis C virus (HCV) circulates as a population of different but closely related genomes: quasispecies nature of HCV genome distribution. J. Virol. 66, 3225–3229.

Murakami, K., Ishii, K., Ishihara, Y., Yoshizaki, S., Tanaka, K., Gotoh, Y., Aizaki, H., Kohara, M., Yoshioka, H., Mori, Y., Manabe, N., Shoji, I., Sata, T., Bartenschlager, R., Matsuura, Y., Miyamura, T., Suzuki, T., 2006. Production of infectious hepatitis C virus particles in three-dimensional cultures of the cell line carrying the genome-length dicistronic viral RNA of genotype 1b. Virology 351, 381–392.

Pawlotsky, J.M., 2006. Hepatitis C virus population dynamics during infection. Curr. Top. Microbiol. Immunol. 299, 261–284.

Perelson, A.S., Herrmann, E., Micol, F., Zeuzem, S., 2005. New kinetic models for the hepatitis C virus. Hepatology 42, 749–754.

Poynard, T., Yuen, M.F., Ratziu, V., Lai, C.L., 2003. Viral hepatitis C. Lancet 362, 2095–2100.

Saito, I., Miyamura, T., Ohbayashi, A., Harada, H., Katayama, T., Kikuchi, S., Watanabe, Y., Koi, S., Onji, M., Ohta, Y., et al., 1990. Hepatitis C virus infection is associated with the development of hepatocellular carcinoma. Proc. Natl. Acad. Sci. U.S.A. 87, 6547–6549.

Shimizu, Y.K., Hijikata, M., Iwamoto, A., Alter, H.J., Purcell, R.H., Yoshikura, H., 1994. Neutralizing antibodies against hepatitis C virus and the emergence of neutralization escape mutant viruses. J. Virol. 68, 1494–1500.

Suzuki, T., Omata, K., Satoh, T., Miyasaka, T., Arai, C., Maeda, M., Matsuno, T., Miyamura, T., 2005. Quantitative detection of hepatitis C virus (HCV) RNA in saliva and gingival crevicular fluid of HCV-infected patients. J. Clin. Microbiol. 43, 4413–4417.

Tagawa, M., Kato, N., Yokosuka, O., Ishikawa, T., Ohto, M., Omata, M., 1995. Infection of human hepatocyte cell lines with hepatitis C virus in vitro. J. Gastroenterol. Hepatol. 10, 523–527.

Wakita, T., Pietschmann, T., Kato, T., Date, T., Miyamoto, M., Zhao, Z., Murthy, K., Habermann, A., Krausslich, H.G., Mizokami, M., Bartenschlager, R., Liang, T.J., 2005. Production of infectious hepatitis C virus in tissue culture from a cloned viral genome. Nat. Med. 11, 791–796.

Zhong, J., Gastaminza, P., Cheng, G., Kapadia, S., Kato, T., Burton, D.R., Wieland, S.F., Uprichard, S.L., Wakita, T., Chisari, F.V., 2005. Robust hepatitis C virus infection in vitro. Proc. Natl. Acad. Sci. U.S.A. 102, 9294–9299.